

Article

Open Ground Story Mid-Rise Buildings Represented by Simplified Systems

José L. Cabrera ¹, Sonia E. Ruiz ^{1,*}  and Amador Teran-Gilmore ²

¹ Instituto de Ingeniería, Universidad Nacional Autónoma de México, CU, Coyoacán, Mexico City 04510, Mexico; jcabreral@iingen.unam.mx

² Departamento de Materiales-Azcapotzalco, Universidad Autónoma Metropolitana, Mexico City 02200, Mexico; tga@uam.azc.mx

* Correspondence: sruizg@iingen.unam.mx

Abstract: An improved methodology for the condensation of Multi-Degree-Of-Freedom (MDOF) systems to equivalent Two-Degree-Of-Freedom (2EDOF) systems is presented. The methodology is applied to mid-rise buildings with Open Ground-Story and verified by means of Nonlinear Time History Analyses. The buildings studied are divided into two main segments: (a) ground story, whose stiffness and lateral strength are both provided only by reinforced concrete moment-resisting frames; and (b) from the second story to the roof, whose stiffness and lateral strength are provided by confined masonry walls. The proposed methodology allows us to do the following: (a) get the closest approximation to the real behavior of the MDOF system through the use of hysteresis rules with strength and stiffness degradation in the simplified system; (b) analyze the behavior of an OGS whose lateral stiffness is lower than the stiffness of the stories above; and (c) identify in which of the two subsystems (either the ground story with reinforced concrete frames or the second story with masonry) the maximum seismic demand of non-linear behavior occurs. For most of the cases studied and different scenarios of non-linear behavior, the 2EDOF simplified system reasonably approximates the MDOF system's response; however, when a local failure in an upper story causes the collapse mechanism, the 2EDOF system does not adequately approximate the response of the MDOF system.

Keywords: buildings with open ground story; confined masonry walls; equivalent two-degree of freedom systems; weak first story buildings; modeling of masonry walls; nonlinear dynamic analysis



Citation: Cabrera, J.L.; Ruiz, S.E.; Teran-Gilmore, A. Open Ground Story Mid-Rise Buildings Represented by Simplified Systems. *Buildings* **2024**, *14*, 1269. <https://doi.org/10.3390/buildings14051269>

Academic Editor: Samir Chidiac

Received: 28 February 2024

Revised: 2 April 2024

Accepted: 6 April 2024

Published: 1 May 2024



Copyright: © 2024 by the authors. Licensee MDPI, Basel, Switzerland. This article is an open access article distributed under the terms and conditions of the Creative Commons Attribution (CC BY) license (<https://creativecommons.org/licenses/by/4.0/>).

1. Introduction

Open Ground-Story buildings are currently one of the most attractive structural systems from the architectural point of view, because they offer a good space/performance combination in zones with limited areas; however, such a structural system presents a strong irregularity in height, which may provoke a deficient structural performance, characterized in most cases by the presence of a Weak First Story (WFS).

The first story of a building with WFS has a discontinuity in lateral stiffness and strength. Thus, the seismic demand for non-linear behavior that causes structural damage tends to concentrate on the first story, provoking excessive damage there that may lead to a sudden structural collapse.

On the other hand, given its vertical irregularity, a structure with OGS may be considered equivalent to a structure with WFS. This means that given its structural properties, the seismic demand will be lower at its upper story than on the ground story; however, an OGS structure is not necessarily a WFS system. In an Open Ground Story-Weak Second Story (OGS-WSS) building, the seismic demand of non-linear behavior located in the ground story tends to move towards the upper stories (primarily at the second story), provoking a concentration of structural damage on that level that may produce a sudden failure. Therefore, if the assumption is that OGS structures always develop a WFS mechanism,

the upper-level seismic demand may be underestimated during the design process. The present study analyzes mid-rise buildings with either a OGS-WFS or, alternatively, with a failure mode on their Second Story (OGS-WSS).

OGS buildings can be analyzed by Nonlinear Time-History Analyses (NTHA); however, analyses of this type may require significant computing time when performing parametric analyses or evaluating seismic structural reliability. This leads to the need for formulating simplified Two-Equivalent-Degree-Of-Freedom systems capable of reproducing the seismic response of Multi-Degree-Of-Freedom buildings.

The fundamental hypothesis of this study is that through the utilization of the improved methodology, simplified equivalent two-degree-of-freedom (2EDOF) systems can be developed to reasonably approach the OGS-WFS and OGS-WSS mechanisms of OGS buildings.

The simplified system is constructed with two degree-of-freedom systems: one representing the lateral behavior of the first story and another for the upper stories. Consequently, by utilizing two degrees of freedom, we aim to offer a reliable alternative that enhances the limitations and capabilities exhibited by one-degree-of-freedom-equivalent systems or by other equivalent systems for finding the seismic response of OGS buildings.

2. Literature Review

2.1. Research on Open Ground Story Buildings

Research on the seismic behavior of buildings whose elevation is irregular has focused on the dynamic analysis of structural frames subjected to lateral loads. In general, the irregularity in the structure has been considered by applying a Modification Factor (MF) to both the stiffness and the lateral strength of its regular version. Chintanapakdee and Chopra [1], Al-Ali and Krawinkler [2], Fragiadakis et al. [3], and Valmudsson and Nau [4] concentrate on the study of irregular plane frames between 5 and 20 stories using NTHA, Modal Nonlinear Pushover Analyses (MNPA), and alternatively, Incremental Dynamic Analyses (IDA). In those studies, the following points are highlighted: (a) in the case of a WFS structure, the irregularity due to stiffness amplifies Interstory Drift Index on the ground story, whereas such Interstory Drift Index is reduced in the rest of the stories; (b) the damage level in an irregular building may be greater than or similar to that in regular structures, depending on both the level of seismic intensity and the characteristics of the irregularity story; (c) MNPA approximates the seismic demand in frames with WFS, while in contrast, NTHA must rigorously determine the seismic structural demand when the ground story is stiffer and stronger than the upper story (named Resistant First Story, RFS).

In Mexico, Ruiz and Diederich [5] perform parametric analyses on buildings of 5 and 12 stories. They conclude that a WFS may occur due to the following: (a) a close relation between the dominant excitation period and that of the structural response; (b) the ratio between the strength of the ground story and the strength of the story above it; (c) the coefficient used for the seismic design. On the other hand, Esteva [6] studied the response of structural systems of 7, 14, and 20 stories, with increased stiffness and strength in the upper levels compared than those in the ground story. According to the author, building non-linear responses are sensitive to the ratio between the upper story lateral shear and the lower story lateral shear.

In most of the research papers listed above, plane structural models (2D) with concentrated plasticity were used. Usually, their nonlinearity was modeled with elastoplastic or bilinear hysteretic behavior. In the present study, it is assumed that the mechanism developed at the first story (reinforced concrete moment-resisting frame) is primarily bending with significant axial load interaction, while the mechanism at the upper stories (masonry) is predominantly governed by shear force. Therefore, a nonlinear modeling based on concentrated plasticity elements with hysteresis models lacking cyclic degradation of stiffness or strength is insufficient in approximating the lateral response in the buildings. Furthermore, vertical irregularity is not obtained by modification factors from the stiffness or lateral resistance of the frame in its regular version; rather, it is explicitly modeled. Consequently,

the lateral response is compromised when considering the degrading interactions between the first and second stories.

2.2. Research on Simplified Equivalent Degree-of-Freedom Systems

Within the framework of seismic-resistant design, it is common to utilize analytical models for evaluating lateral behavior and the stability of structural systems. Taking into account the specified requirements, the degree of model refinement may become significant, and in many cases, conducting a series of detailed seismic analyses becomes necessary to obtain the model's response. In this context, the development of simplified models that replicate the response of refined analytical models becomes essential.

The primary objective of a simplified model is to produce results similar to those obtained from the refined model while maintaining low computational demands and offering the ability to have a greater parametric range. This objective has been studied by many researchers who have developed analytical models that address their needs and have proposed its simplification based on the lateral response in the elastic and inelastic ranges.

Procedures for the evaluation of the lateral buildings response have been proposed considering the results obtained from Nonlinear Pushover Analyses. Fajfar and Gašperšič [7] propose a method named N2, which centers on approximating the response of a real MDOF system using a One-Degree-of-Freedom-Equivalent system with initial stiffness and elasto-plastic hysteresis, evaluating the displacement demand using inelastic spectra. Afterward, this method is extended to consider the torsional effects in buildings with irregular floor plans.

Dolšek and Fajfar [8] propose a method for the probabilistic evaluation of irregular structures in a plan, named IN2. This method is considered a simplified alternative to Incremental Dynamic Analysis, IDA, due to its easy implementation and the degree of prediction it offers. Three-story reinforced concrete buildings with irregular floor plans were analyzed using the method. According to the results of this study, the IN2 method is suitable for evaluating asymmetric buildings.

Ruggieri et al. [9] propose a methodology for condensing mid-rise buildings with irregular floor plans into simplified systems with n degrees of freedom. In their method, the horizontal and vertical elements of the MDOF building are condensed into a series of rectangular or quadrangular elements named Travolino. The methodology is applied to 15 reinforced concrete (R/C) buildings with irregular floor plans of 2 and 3 stories. From Nonlinear Pushover Analyses performed on real buildings, the hysteresis parameters of the Travolino models are calibrated and later used in a series of IDAs. Their results indicate that the response of Travolino models adequately coincides with that of buildings within the linear and nonlinear range.

As a result of this study, it was found that the Travolino model accurately captures the effect of horizontal irregularities in the asymmetric-plan buildings. This improvement in accuracy is achieved by utilizing 1DOF systems, resulting in reduced computational requirements for performing IDAs on MDOF buildings.

Lin and Tsai [10] study irregular Multi-Degree-of-Freedom (MDOF) buildings in plan. Based on the capacity curves obtained from Nonlinear Pushover Analyses in these irregular buildings, the MDOF systems are condensed into Two-Degree-of-Freedom systems. The simplified systems account for the torsional moment floor rotation relationship in asymmetric MDOF systems using a mass eccentricity placed at one end of the element with a rotational spring. The results indicate a better approximation of the translational response as well as the rotational response of MDOF buildings.

Bakalis et al. [11] study the design simplification and lateral response assessment of liquid storage tanks. They consider that the tank's base plate can be discretized into rigid beams. Each beam incorporates a tension-free elastic spring to represent soil stiffness, and this simultaneously takes into account the phenomenon of base plate uplift. The "joystick model" simplified system is constructed with an elastic bar with a concentrated mass at its upper end. The lower end of this bar is connected to rigid beams that simulate the base plate.

The simplified methodology is based on Nonlinear Pushover Analyses, and its evaluation is performed by executing IDAs. Establishing a damage threshold demonstrates that the simplified methodology reasonably approximates the elastoplastic buckling damage observed at the tank's lower perimeter. The results obtained from IDA and pushover fragility curves indicate that the methodology can be used in a design code, providing conservative results and reducing computation time in nonlinear analyses with finite elements.

In the context of buildings, the One-Equivalent-Degree-Of-Freedom model is frequently used to estimate lateral deformation under seismic actions. Many research projects have been conducted to determine its properties (linear and non-linear), most of them centered on regular MDOF buildings and in some cases on buildings with vertical irregularities.

Fajfar and Gašperšič [7] propose the use of the N2 method in the condensation of concrete buildings with Weak First Story to One-Equivalent-Degree-Of-Freedom systems. The results derived from this study indicate that analyses using the N2 method can provide reasonably accurate predictions of global lateral displacement demand compared to those obtained from Nonlinear Time History Analyses with MDOF systems. Therefore, the study indicates that the proposed 1EDOF system can adequately detect the formation of a WFS mechanism.

Kuramoto et al. [12] propose a methodology based on the capacity spectrum for the transformation of irregular buildings into 1EDOF simplified systems. Regular 6-, 10-, and 19-story reinforced concrete frames and 5-, 10-, and 20-story structural steel frames are studied, considering three cases of irregularity: WFS, RFS, and Weak Story (WS). Both MDOF systems and simplified systems are subjected to Nonlinear Time History Analyses. Using such systems, lateral Interstory Drift Index demands can be approximated reasonably; however, for tall buildings (19 and 20 stories) with RFS, the 1EDOF system is incapable of reproducing results when an upper story deforms much more.

The 1EDOF system can be used to predict the response of both regular and irregular buildings; however, in the present study, the sudden change in elevation is defined both by elements that are highly degraded when subjected to seismic motions (masonry walls on the upper stories) and by elements that have less stiffness on the ground story; therefore, a 1EDOF model cannot be applied in the solution of such structural systems.

For restoring force characteristics of the complete system and its structural components, the 1EDOF system uses only one capacity curve and one hysteretic rule; however, only one capacity curve and one hysteretic rule are not enough to adequately describe the response of a system with different structural elements, hence the need to assign, in the present study, a first degree of freedom to the first story and a second degree of freedom to the upper stories. Thus, we consider that 2EDOF systems are necessary to reproduce the response of MDOF systems with vertical irregularity (with OGS) as accurately as possible, considering the non-linear interaction between the two types of substructures.

Xu and Yuan [13] analyze buildings with vertical irregularity with two types of substructures: lower stiff structure and flexible upper structure. It is considered that MDOF systems can be condensed to 2EDOF systems by means of an empiric process. This is done by evaluating a factor called α_{ii} , which defines the interaction between the lower and upper structures in terms of mass, stiffness, and the seismic force.

Tena and Hernández [14] condense a MDOF system into a 2EDOF system through a calibrated curve with simulations of two-degree-of-freedom systems. The curve is built with the statistical properties of MDOF systems with WFS. The 2EDOF system is obtained by entering the period, mass, and target stiffness of a regular system into the calibrated curve. Then, parametric analyses are performed with such simplified 2EDOF systems, assuming perfect elastoplastic hysteretic behavior. A reasonable approximation for the comparison of responses is reported in terms of the displacement between the real MDOF building and its corresponding simplified system.

Lin et al. [15] propose a method for converting MDOF buildings with vertical irregularity to simplified Two-Equivalent-Degree-Of-Freedom systems by adopting the capacity spectrum method. The methodology is applied to structural steel buildings divided into two substructures: (a) stiff/resistant lower structure, and (b) weak/flexible upper structure.

A series of Nonlinear Time History Analyses are conducted on MDOF buildings and their corresponding simplified systems. Their study indicates that the 2DOF system provides a better approximation for the Interstory Drift Index of the upper structure in the MDOF system compared to a 1DOF system, since the superposition of its modal response does not align with the deformed configuration of the upper structure in the MDOF system, which is less rigid and less resistant than the lower structure.

3. General Methodology

In the present study, the methodology by Lin et al. [15] is improved as follows: (a) modifications to the spectral capacity method curves are introduced to include the analysis of buildings with OGS-WSS as well as of buildings with OGS-WFS; (b) hysteretic rules are introduced, taking into account degradation of both stiffness and strength, in order to better approximate the nonlinear seismic response of MDOF systems; (c) the methodology is applied to buildings with a reinforced concrete (R/C) moment-resisting frame in the OGS and confined masonry walls in the upper stories. It is noticed that these considerations are not implemented in reference [15], and we apply it to mid-rise OGS buildings with mechanical properties like those that have failed in Mexico City during intense earthquakes.

The 2EDOF system methodology presented here is a more complete alternative compared to the other simplified methodologies mentioned in this study (Section 2.2 for vertical irregularities); some improvements are mentioned above.

The improved methodology is applicable to buildings that fulfil the following: (a) they have a response dominated by the first mode of vibration; (b) they are regular in plan; (c) buildings in which lateral deformation is controlled by global shear deformation; (d) they have WFS or WSS as structural failure mechanisms, which are described as follows:

- Case I, mechanism OGS-WSS: Building with vertical irregularity, where the maximum Interstory Drift Index is located at the upper stories.
- Case II, mechanism OGS-WFS: Building with vertical irregularity, where the maximum Interstory Drift Index is located at the first story.

For both mechanisms, it is considered that the lateral stiffness at the first story is lower than at the upper stories and that the lateral resistance at the first story can be greater or smaller than at the upper stories.

Figure 1 illustrates the general methodology used for the condensation of MDOF systems into 2EDOF systems. This is divided into three parts: (1) analysis of MDOF systems; (2) condensation of 2EDOF simplified systems; and (3) verification of seismic responses.

In the subsequent sections, the steps outlined in the proposed methodology are discussed.

3.1. First Part—Modeling and Nonlinear Analysis of MDOF Systems

In this section, the type of nonlinear modeling to be used in the concrete frames and masonry walls is described.

This methodology acknowledges that in the nonlinear modeling of these types of buildings, the capacity and stability of the columns may be compromised due to axial compressive loads and the discontinuity at the top of the element. The theory of small deformations is not acceptable because of the substantial displacements induced by seismic forces in combination with vertical loading (geometric nonlinearity). Therefore, as we will see later, this methodology does not permit the use of concentrated plasticity elements constructed with moment curvature/rotation envelopes in reinforced concrete columns in systems with WFS (Case I).

A three-dimensional nonlinear model is constructed to perform a series of Modal Nonlinear Pushover Analyses and Nonlinear Time History Analyses. A MNPA should be performed for each vibrational mode that significantly contributes to the overall response of the building. The analysis will be conducted in a specific direction of interest and will consider a lateral load pattern proportional to the modal shape of the n -th mode. Then, a NTHA is executed in the same direction of interest, obtaining the system response in terms of Interstory Lateral Displacement and Interstory Drift Index.

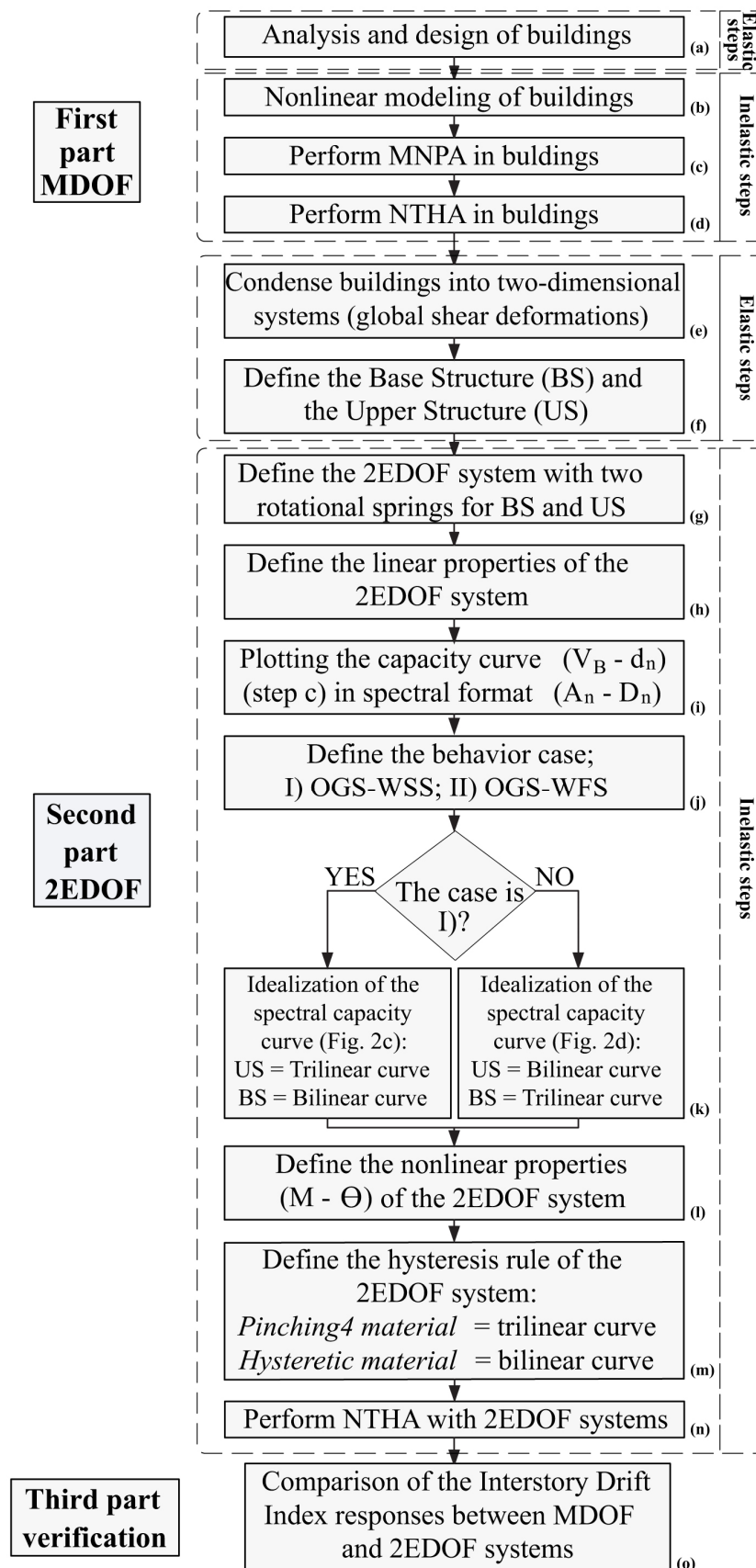


Figure 1. General methodology.

3.2. Second Part—Condensation of 2EDOF Simplified Systems

3.2.1. Shear-Type MDOF System Division

Considering lateral deformation in MDOF systems governed by global shear deformations, it becomes feasible to statically condense degrees of freedom in three-dimensional systems, resulting in an equivalent system of concentrated masses with one degree of freedom per level. This facilitates the identification of stiffness submatrices when the MDOF system is divided.

The simplified system is built with the dynamic properties of the original irregular MDOF system, dividing it into two sections: (a) Base Structure (BS), which is defined as from the base of the building (ground) to the story in which the vertical irregularity is located; and (b) Upper Structure (US), which is defined as from the upper part of the BS to the roof. BS and US are schematically shown in Figure 2a.

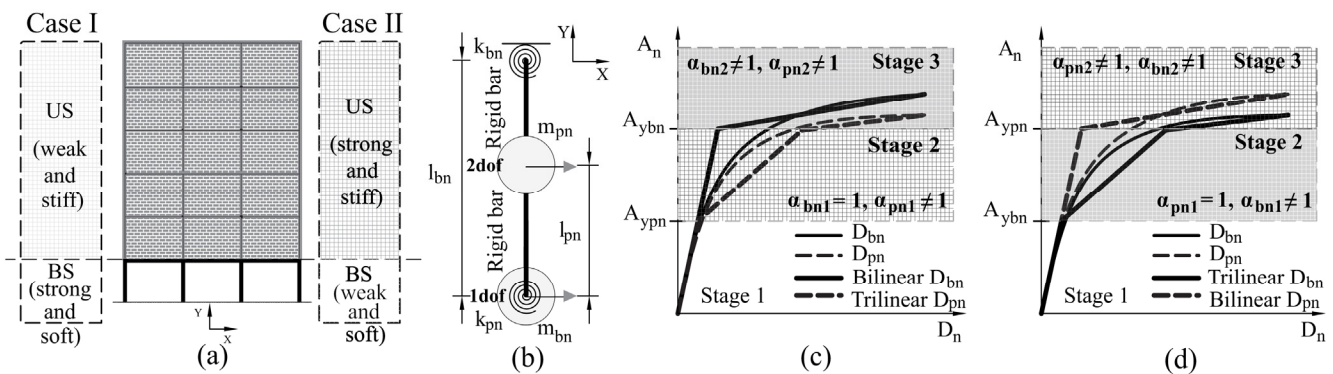


Figure 2. Transformation methodology, (a) division of the MDOF system; (b) 2EDOF system [15]; (c) capacity curves, Case I; (d) capacity curves, Case II.

3.2.2. Simplified 2EDOF System

The 2EDOF model is shown in Figure 2b, and it is structured by two rigid bars; the upper bar has a length l_{pn} , and the lower bar has a length l_{bn} . The system has two concentrated masses in the final part of each bar, named m_{pn} and m_{bn} , and considers two springs with rotational stiffness, located at the beginning of both the pn -bar and the bn -bar, named k_{pn} and k_{bn} , respectively. The length of the pn -bar is fixed at 1 with a positive orientation, and the length of the bn -bar is considered negative; in other words, the lower rigid bar must be oriented downward [15].

The negative orientation of the bn -bar is necessary so that, within the elastic range, the concentrated masses m_{pn} and m_{bn} remain in a single vertical line when pushed laterally. In other words, the displacement $D_{pn} = D_{bn}$ and rotation $\theta_{pn} = \theta_{bn}$ conditions necessary for the 2EDOF system to exhibit the same response as a 1EDOF system within the elastic range are satisfied.

3.2.3. Equations Governing the Seismic Behavior of MDOF and 2EDOF Systems

The general equation of motion for the elastic case of both subsystems (BS and US) is expressed as follows:

$$M\ddot{u} + C\dot{u} + Ku = -M\ddot{u}_g(t) \tag{1}$$

where

$$u = \begin{bmatrix} u_p \\ u_b \end{bmatrix}_{N \times 1}, \quad M = \begin{bmatrix} m_p & 0 \\ 0 & m_b \end{bmatrix}_{N \times N}, \quad K = \begin{bmatrix} k_{pp} & k_{pb} \\ k_{bp} & k_{bb} \end{bmatrix}_{N \times N}, \quad C = \begin{bmatrix} c_{pp} & c_{pb} \\ c_{bp} & c_{bb} \end{bmatrix}_{N \times N} \tag{2}$$

where $[M]$, $[C]$, and $[K]$ are the matrices of mass, damping, and stiffness of the divided MDOF system. The vector $\{u\}$ represents the response with respect to the displacements of US and BS. In each matrix, N is the number of elements, subscript p refers to the US, and subscript b refers to the BS. Equation (1) may be adjusted to incorporate the modal shape

$\{\varphi_n\}$ for the vibration n -th mode, enabling us to analyze the distinct behaviors of US and BS. The modal shape vector is defined by the following:

$$\varphi_n = \begin{Bmatrix} \varphi_{pn} \\ \varphi_{bn} \end{Bmatrix} \quad (3)$$

where φ_{pn} is the modal shape of the US and φ_{bn} is the modal shape of the BS. In this way, the motion equation is reorganized to transform the dynamic properties of the MGD system into dynamic properties of two degrees of freedom. Assuming this, it is possible to transform vector φ_{pn} into a modal matrix for the vibration n -th mode, as in Equation (4), which contains the modal column vectors ($\{\varphi_{pn}\}, \{\varphi_{bn}\}$) for the BS and US. Similarly, Equation (5) expresses the connection between the matrix and vector in modal form, where 1 represents a vector with dimensions 2×1 , and all elements are equal to 1.

$$\varphi_n^d = \begin{bmatrix} \varphi_{pn} & 0 \\ 0 & \varphi_{bn} \end{bmatrix}_{N \times 2} \quad (4)$$

$$\varphi_n = \varphi_n^d \{1\} \quad (5)$$

Therefore, the response of the 2EDOF system for the vibration n -th mode is defined as follows:

$$D_n(t) = \begin{bmatrix} D_{pn}(t) \\ D_{bn}(t) \end{bmatrix}_{2 \times 1} \quad (6)$$

where D_{bn} and D_{pn} are the equivalent displacements of the BS and the US, respectively. The relationship between the response of the divided MDOF system and the simplified 2EDOF system can be expressed as follows:

$$u_n(t) = \begin{bmatrix} u_{pn}(t) \\ u_{bn}(t) \end{bmatrix} = \begin{bmatrix} \varphi_{pn} D_{pn}(t) \\ \varphi_{bn} D_{bn}(t) \end{bmatrix} = \begin{bmatrix} \varphi_{pn} & 0 \\ 0 & \varphi_{bn} \end{bmatrix} \cdot \begin{bmatrix} D_{pn}(t) \\ D_{bn}(t) \end{bmatrix} = \Gamma_n [\varphi_n^d] \{D_n(t)\} \quad (7)$$

where Γ_n is the modal participation factor corresponding to the vibration n -th mode. Therefore, the linear dynamic equation of motion of the 2EDOF system is as follows:

$$\tilde{M}_n \{\ddot{D}_n(t)\} + \tilde{C}_n \{\dot{D}_n(t)\} + \tilde{K}_n \{D_n(t)\} = -\tilde{M}_n \{1\} \ddot{u}_g(t) \quad (8)$$

where

$$\tilde{M}_n = [\varphi_n]^T [M] [\varphi_n] = \begin{bmatrix} \varphi_{pn}^T \cdot m_p \cdot \varphi_{pn} & 0 \\ 0 & \varphi_{bn}^T \cdot m_b \cdot \varphi_{bn} \end{bmatrix}_{2 \times 2} \quad (9)$$

$$\tilde{C}_n = [\varphi_n]^T [C] [\varphi_n] = \begin{bmatrix} \varphi_{pn}^T \cdot C_{pp} \cdot \varphi_{pn} & \varphi_{pn}^T \cdot C_{pb} \cdot \varphi_{pn} \\ \varphi_{pn}^T \cdot C_{bp} \cdot \varphi_{pn} & \varphi_{pn}^T \cdot C_{bb} \cdot \varphi_{pn} \end{bmatrix}_{2 \times 2} \quad (10)$$

$$\tilde{K}_n = [\varphi_n]^T [K] [\varphi_n] = \begin{bmatrix} \varphi_{pn}^T \cdot k_{pp} \cdot \varphi_{pn} & \varphi_{pn}^T \cdot k_{pb} \cdot \varphi_{pn} \\ \varphi_{pn}^T \cdot k_{bp} \cdot \varphi_{pn} & \varphi_{pn}^T \cdot k_{bb} \cdot \varphi_{pn} \end{bmatrix}_{2 \times 2} \quad (11)$$

Matrices $[\tilde{M}_n]$, $[\tilde{C}_n]$, and $[\tilde{K}_n]$ correspond to the divided MDOF system for the vibration n -th mode considering two degrees of freedom.

3.2.4. Elastic and Inelastic Properties of 2EDOF Systems

The simplified system's mass is considered equal to the mass matrix \tilde{M}_n of the MDOF system with two degrees of freedom for the vibration n -th mode; thus, $m_{pn} = \tilde{M}_{n1,1}$ and $m_{bn} = \tilde{M}_{n2,2}$. On the other hand, the simplified stiffness k is derived from stiffness analysis using the simplified system; by equating matrix k with matrix (11), it is deduced that the simplified stiffnesses in the linear range are $k_{pn} = \tilde{K}_{n1,1} = \varphi_{pn}^T \cdot k_{pp} \cdot \varphi_{pn}$ and

$k_{bn} = l_{bn}^2 \cdot \left(\varphi_{pn}^T \cdot k_{bb} \cdot \varphi_{pn} - \frac{(\varphi_{pn}^T \cdot k_{pb} \cdot \varphi_{pn})^2}{\varphi_{pn}^T \cdot k_{pp} \cdot \varphi_{pn}} \right)$, where k_{pn} represents the elastic stiffness of the upper spring corresponding to the US and k_{bn} represents the elastic stiffness of the lower spring corresponding to the BS.

The non-linear properties of the 2EDOF system are obtained assuming that the maximum response under dynamic excitation can be obtained through an MNPA in the MDOF system, obtaining capacity curves ($V_B - d_n$) which define the displacement of the US/BS and the basal shear. Using the following expressions, capacity curves need to be converted into a spectral format:

$$D_{bn} = \frac{d_{n,tb}}{\Gamma_n \phi_{n,tb}}, D_{pn} = \frac{d_{n,tp}}{\Gamma_n \phi_{n,tp}}, A_n = \frac{V_B}{\Gamma_n^2 M_n}, \quad (12)$$

where M_n , $u_{n,tb}$, $u_{n,tp}$, $\varnothing_{n,tb}$, and $\varnothing_{n,tp}$ are effective modal mass, displacement in the upper part of the BS, displacement in the upper part of the US, modal form of the BS, and modal form of the US, respectively. A_n represents the spectral acceleration for the vibration n -th mode.

The capacity curves give information about the following:

- The behavior case: (I) OGS-WSS or (II) OGS-WFS.
- The restoring forces of the 2EDOF system.

The choice between Case I or II depends on the subsystem where the maximum Inter-story Drift Index (IDI) occurs. When IDI occurs in the US, the behavior corresponds to Case I, but to Case II if IDI occurs in the BS. The IDI value corresponds to the formation of a collapse mechanism; therefore, it should be calculated using the final load step.

The restoring forces of the 2EDOF system are determined by idealizing the capacity curves in spectral format $A_n - D_n$ into curves in bilinear and/or trilinear format. Figure 2c,d shows the bilinear and/or trilinear envelopes that govern the nonlinear behavior of buildings in Cases I and II, respectively. Considering the characteristics of these curves, their lateral structural behavior simplifies into the following three stages:

- Stage 1: the behavior is elastic in both springs; the response of the 2EDOF system is equivalent to the response of a 1EDOF system.
- Stage 2: the behavior is non-linear because one of the springs (US or BS) reaches the non-linear range with its corresponding post-yield stiffness, k'_n in a trilinear envelope. The other spring remains elastic.
- Stage 3: the elastic spring (stage 2) reaches the non-linear range with its corresponding post-yield stiffness k'_n , in a bilinear envelope. The other spring is still in the non-linear range with its second post-yield stiffness k''_n , following its trilinear envelope.

The inelastic stiffnesses for the upper and lower springs in stages 2 and 3 of the 2EDOF model are determined based on the post-yield slopes (α) of the idealized curves and on the solution of the equation of flexibility (13), which is expressed in terms of displacement D_n .

$$\varepsilon \begin{pmatrix} D_{pn} \\ D_{bn} \end{pmatrix} = \delta \begin{bmatrix} \frac{m_{pn}}{k'_{pn}} + \frac{m_{bn} \left(1 + \frac{1}{l_{bn}}\right) + m_{pn} \left(1 + \frac{1}{l_{bn}}\right)^2}{\frac{k'_{bn}}{l_{bn}^2}} \\ \frac{m_{bn} + m_{pn} \left(1 + \frac{1}{l_{bn}}\right)}{\frac{k'_{bn}}{l_{bn}^2}} \end{bmatrix} \quad (13)$$

As the bar transits into the inelastic phase (stage 2), the flexibility matrix of Equation (13) changes so that an increase in δ results in an increase in displacement ε . Considering the behavior stages, the inelastic stiffnesses k_n for Cases I and II are as follows:

Stage 1

$$k'_{pn} = \frac{m_{pn}}{\frac{m_{pn}}{k_{pn}} + \frac{m_{bn} \left(1 + \frac{1}{l_{bn}}\right) + m_{pn} \left(1 + \frac{1}{l_{bn}}\right)^2}{\frac{k_{bn}}{l_{bn}^2}}} - \frac{m_{bn} \left(1 + \frac{1}{l_{bn}}\right) + m_{pn} \left(1 + \frac{1}{l_{bn}}\right)^2}{\frac{k'_{bn}}{l_{bn}^2}}$$

$$k'_{bn} = \alpha_{bn1}(k_{bn})$$

(14)

Stage 2

$$k''_{pn} = \frac{m_{pn}}{\frac{m_{pn}}{k_{pn}} + \frac{m_{bn} \left(1 + \frac{1}{l_{bn}}\right) + m_{pn} \left(1 + \frac{1}{l_{bn}}\right)^2}{\frac{k_{bn}}{l_{bn}^2}}} - \frac{m_{bn} \left(1 + \frac{1}{l_{bn}}\right) + m_{pn} \left(1 + \frac{1}{l_{bn}}\right)^2}{\frac{k''_{bn}}{l_{bn}^2}}$$

$$k''_{bn} = \alpha_{bn2}(k_{bn})$$

where α_{pn1} and α_{pn2} correspond to the post-yielding slopes of the pn -bar capacity curve at stages 1 and 2, respectively. The slopes α_{bn1} and α_{bn2} are associated with the bn -curve at the same stages. In the methodology presented here, we propose to modify the value of the post-flow slope α_{pn} that governs the behavior stages of the idealized curve of the pn -bar to include the WFS failure mechanism. In the methodology, the pn curve represents the lateral behavior of the US in the MDOF system, and for the WFS mechanism, the US must remain elastic or with little lateral deformation. Therefore, a value of $\alpha_{pn} = 1$ is assumed in the pn curve shown in Figure 2d, indicating that the US in the 2EDOF system remains linear, once the BS yields. On the other hand, the slope of the bn -curve is different from unity, which indicates the yielding of the bn -bar.

Finally, the hysteresis of the 2EDOF system is defined by the moment M_{yn} and the rotation θ_{yn} of the upper and lower springs. These moments indicate the yielding of the pn and bn bars at different stages in the capacity curves. Therefore, these are calculated with the A_{yn} breakpoint points using the following expressions:

Stage 1

$$\begin{aligned} M_{y_{pn1}} &= A_{y_{pn1}}(m_{pn}) \\ M_{y_{bn1}} &= A_{y_{bn1}}[(1 + l_{bn})m_{pn} + l_{bn}(m_{bn})] \end{aligned} \quad (15)$$

Stage 2

$$\begin{aligned} M_{y_{pn2}} &= A_{y_{pn2}}(m_{pn}) \\ M_{y_{bn2}} &= A_{y_{bn2}}[(1 + l_{bn})m_{pn} + l_{bn}(m_{bn})] \end{aligned} \quad (16)$$

3.2.5. Hysteretic Rules for the Simplified 2EDOF System

In the present study, trilinear and bilinear hysteresis rules are applied, which differ from those used in the publications related with 2DOF equivalent nonlinear systems mentioned above [10,15]. With the aim to improve the accuracy of the MDOF system response,

the hysteresis rules used herein include both stiffness (δ_K) and strength deterioration (δ_R). The rules were selected to explicitly consider the case where the structural members on the first level of an irregular building exhibit different linear and nonlinear behavior than those on the second story (a scenario studied in this study).

The bilinear and trilinear rules used in the Nonlinear Time History Analyses correspond to the Hysteretic and Pinching4 rules, respectively. Hysteresis cycle parameters are found in the Open System for Earthquake Engineering Simulation (OpenSees) [16] software library (version 3.2.2). These parameters were integrated into a numerical routine for solving Equation (1). Figure 3 shows the hysteresis backbone for both rules, as well as the parameters utilized in this study to regulate the hysteretic cycles.

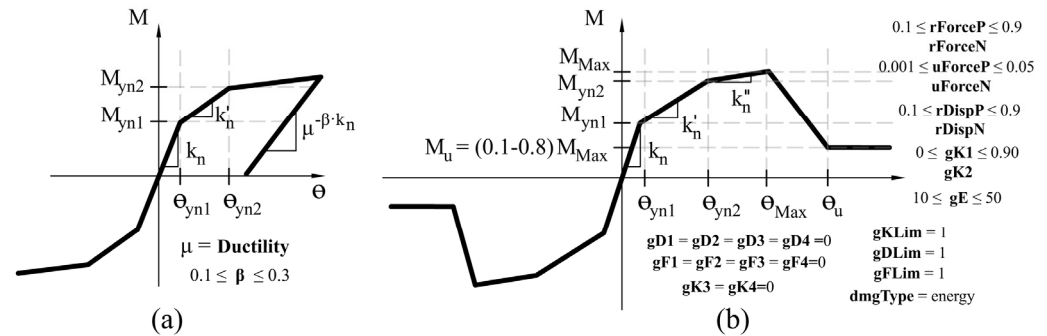


Figure 3. Hysteretic rules adapted from [16], (a) Hysteretic; (b) Pinching4.

A trilinear Pinching4 rule with δ_K and δ_R is used in the spring that first reaches the non-linear range, and a bilinear Hysteretic rule with only δ_K for the other spring. To simulate the strength loss in the first spring, an ultimate rotation value θ_u is used at the last point of the backbone (descending branch with negative slope) of the Pinching4 rule, as a percentage of the rotation associated with the maximum resistance reached, θ_{Max} . The value θ_u should be calibrated empirically in each case study.

3.3. Third Part—Comparison of the Responses of MDOF and 2EDOF Systems

In accordance with the general methodology, OpenSees software (version 3.2.2) is used to perform a series of Nonlinear Time History Analyses on simplified systems using non-linear hysteretic rules.

4. Application of the Methodology to OGS Buildings

Part 1 of the general methodology is developed in this section. The non-linear seismic responses of mid-rise buildings with OGS are obtained using a series of Nonlinear Time History Analyses with seismic motions recorded in Mexico City. The structuring of the buildings is similar to that of some buildings that collapsed during the Mexico earthquake of 19 September 2017 (19S-2017). In the second part of the general methodology, MDOF systems are condensed into 2EDOF simplified systems. Later, a comparison between both systems responses is performed in the third part.

4.1. Description of Case Studies

The buildings studied are divided into two main segments: (a) ground story, whose stiffness and lateral strength are both provided only by reinforced concrete (R/C) moment-resisting frames; and (b) from the second story to the roof, whose stiffness and lateral strength are provided by confined masonry walls (MW) and both vertical and horizontal reinforced concrete elements (R/C tie columns and R/C tie beams). The height of each story is 2.5 m, except for the ground floor, the height of which is 2.8 m. The structure has 5 bays in the X direction, and 3 bays in the Y direction. The structure's long side is 15 m, and its short side is 10 m. The buildings analyzed have 3, 5, and 7 stories. Figure 4 shows the building plan view, together with three schematic elevation views that indicate both the

total height and its structural configuration. Due to architectural design, masonry walls are distributed the same on all levels. Consequently, section walls and confined R/C members (tie columns, beams) remain constant.

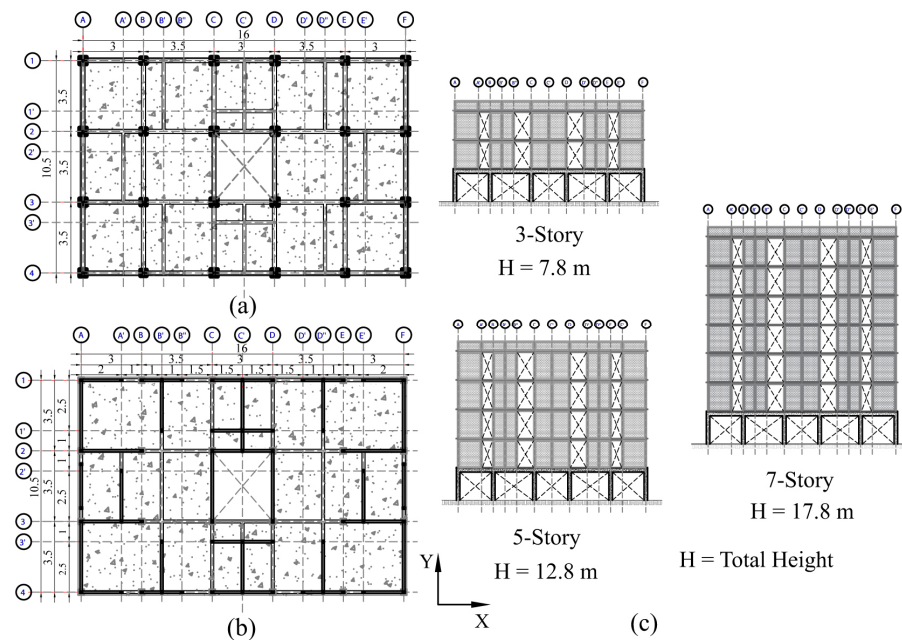


Figure 4. Plan and elevation view of structural elements; (a) ground story; (b) second story–roof; (c) total height, H.

As a result of the different mechanical properties of the masonry units, different stiffness and strength ratios are determined between the ground story and the second story. Five cases are assumed for the masonry: (P1) solid fired clay brick, which is considered a low-strength piece; (P2) hollow concrete block, which is a low-strength piece; (P3) smooth, perforated concrete block, which is a high-strength piece; (P4) solid clay brick with horizontal reinforcement in joints, which is a low-strength piece; and (P5) smooth, perforated concrete block with horizontal reinforcement, which is a high-strength piece. The mechanical properties of the pieces are shown in Table 1, where t , l , and h refer to the pieces' thickness, length, and height, respectively.

Table 1. Mechanical properties of masonry.

Case	Dimensions $t \times l \times h$ (m)	f'_m (MPa)	v'_m (MPa)	E_m (MPa)	G_m (MPa)
P1	0.12 × 0.24 × 0.06	2.7	0.25	714.4	475.6
P2	0.15 × 0.40 × 0.20	3.8	0.28	3955.3	1939.9
P3	0.12 × 0.24 × 0.12	6.9	0.86	4930.7	986.2
P4	0.12 × 0.24 × 0.06	2.4	0.24	654.6	377.1
P5	0.12 × 0.24 × 0.12	9.3	0.91	5971.7	1194.3

The compression strength f'_m , modulus of elasticity E_m , diagonal compression strength v'_m , and shear modulus G_m are representative of values obtained from laboratory tests carried out in Mexico on masonry pieces commercially available in Mexico City. The low-/high-strength classification refers only to the mechanical properties rather than design regulations.

The building is symmetrical in plant view, and it is assumed that the concrete slab floor system works as a rigid diaphragm. The buildings were both analyzed and designed according to the Mexico City Building Code 2017 [17] and its Supplementary Technical Regulations for Seismic Design 2020 [18]. The numerical model was created using commercial software. In structural modeling, frame type elements were used to represent concrete elements; masonry walls were modeled using the wide column methodology [19].

Seismic behavior factor $Q = 2$ was considered in all cases for the structural analysis and design. This was except for cases P2, in which the value of Q was 1.5.

For structural analysis and design, a seismic behavior factor $Q = 2$ was considered for solid masonry pieces, and a factor $Q = 1.5$ for hollow masonry pieces.

The value of Q is selected according to both the deformation capacity of the system and the masonry piece classification (hollow/solid) assigned by the Regulations for Seismic Design [18]. Both the elastic pseudo acceleration spectra and the reduced pseudo acceleration spectra for seismic design are shown in Figure 5, where T is the period and S_a/g is the pseudo acceleration, normalized to gravity, g .

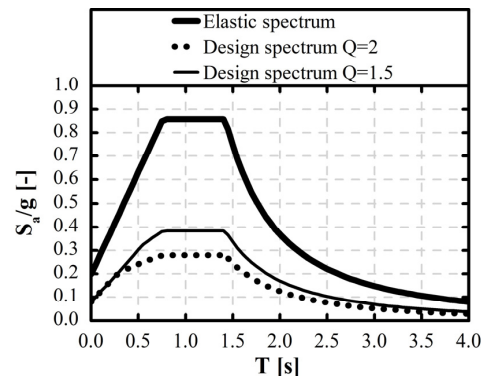


Figure 5. Elastic spectra and seismic design spectra.

The Supplementary Technical Regulations for Seismic Design 2020 indicate that the Interstory Drift Index value for the Collapse Prevention Limit State (CPLS) must be limited to a value corresponding to exceeding the story deformation capacity, called the Maximum Permissible Interstory Drift Index (MPIDI). The CPLS objective is that, for the design intensity (S_{aD}/g), the drift of all stories must not exceed its lateral deformation capacity.

Two MPIDI values are used in the present study because the structuring is mixed in elevation. Table 2 shows the values of analysis and structural design for the case studies. It also shows the first two periods (T_1, T_2) in direction X , with their respective participation Mass Ratios (MR). The periods shown were calculated based on the design concrete and masonry strengths.

Table 2. Design properties of the case studies.

Stories	T_1 (s)	MR	T_2 (s)	MR	Q	MPIDI		SaD/g
						R/C Frame	Masonry Walls	
Masonry P1								
3	0.36	0.99	0.36	0.01	2	0.015	0.005	0.22
5	0.40	0.95	0.37	0.05				0.22
7	0.47	0.84	0.42	0.16				0.24
Masonry P2								
3	0.30	0.99	0.29	0.01	1.5	0.015	0.004	0.21
5	0.33	0.95	0.31	0.05				0.23
7	0.42	0.82	0.34	0.18				0.26
Masonry P3								
3	0.28	0.99	0.28	0.01	2	0.015	0.005	0.20
5	0.33	0.92	0.30	0.08				0.21
7	0.42	0.80	0.35	0.10				0.23
Masonry P4								
3	0.37	0.99	0.36	0.01	2	0.015	0.01	0.22
5	0.40	0.94	0.38	0.06				0.22
7	0.48	0.83	0.43	0.17				0.24
Masonry P5								
3	0.38	0.99	0.38	0.01	2	0.015	0.01	0.22
5	0.40	0.96	0.37	0.04				0.22
7	0.45	0.87	0.39	0.13				0.23

According to Supplementary Technical Regulations for Concrete Design, strong column-weak beam was used for designing the reinforced concrete frames. The resulting transverse and percentage of transverse steel of the columns are shown in Table 3.

Table 3. Dimensions of reinforced concrete columns.

Case	3-Story		5-Story		7-Story	
	Dimensions	A_s/A_g (%)	Dimensions	A_s/A_g (%)	Dimensions	A_s/A_g (%)
P1	0.30 × 0.30	3.1, 3.5	0.35 × 0.35	3.5	0.40 × 0.40	2.6
P2	0.35 × 0.35	2.2	0.40 × 0.40	2.2	0.45 × 0.45	2.7
P3	0.35 × 0.35	2.8	0.40 × 0.40	1.7	0.45 × 0.45	3.0
P4	0.30 × 0.30	4.5	0.35 × 0.35	3.5	0.40 × 0.40	2.7
P5	0.30 × 0.30	4.5	0.35 × 0.35	3.5	0.40 × 0.40	3.8

4.2. Non-Linear Buildings Modeling

The tridimensional MDOF systems are analyzed with OpenSees software (version 3.2.2). For the numerical solution of Equation (1), the Newmark average acceleration method is used, with a diagonal mass matrix and a damping matrix given by the Rayleigh model. A critical damping percentage of 5% is considered in the first two vibration modes in the X direction (see Figure 4). The P-Delta effects are included in the reinforced concrete columns, and the base supports are totally restrained.

4.2.1. Modeling of R/C Frames

The reinforced concrete elements (beams and columns) in the frame system are modeled using distributed plasticity force-based elements with 5 Gauss–Lobatto integration points. The transverse section is discretized into fibers, which use concrete and steel constitutive relations of define their non-linearity. The uniaxial material Concrete02 defines concrete's stress–strain curve. For column-type elements, three confinement levels are used, following Ezequiel [20]: confined concrete, partially confined concrete, and unconfined concrete. For beam-type elements, only unconfined concrete is used. The concrete constitutive relation is built using the Mander model [21]. Concrete rebar is modeled with uniaxial Steel02 Giuffrè–Menegotto–Pinto material, strain hardening elastoplastic model. The constitutive relation of reinforcing steel is built using Rodriguez and Botero's [22] values.

4.2.2. Modeling of Masonry Walls

A beam-truss model by Panagiotou et al. [23,24] is used to represent non-linear behavior in confined masonry walls. The idealization of masonry is archived through a geometric arrangement of vertical, horizontal, and diagonal elements forming a quadrangular or rectangular perimeter, which is referred to as a panel in this study. The beam-truss model was developed mainly for non-linear modeling of reinforced concrete walls; however, studies performed by Williams [25], Ayala [26], and Moharrami et al. [27], demonstrate the use of such models in confined masonry walls and diaphragm walls.

ConcretewBeta is the uniaxial material that represents the constitutive relationship of masonry and concrete in the panel element. Steel02 material is the constitutive relation of rebar in tie columns. The uniaxial material Steel01, whose hysteretic behavior is elastoplastic, is used to represent the horizontal reinforcing steel present in the masonry joints in cases P4 and P5 (see Table 1).

The vertical elements that represent both the masonry and the tie columns are modeled using distributed plasticity force-based elements with 2 Gauss–Lobatto integration points. The horizontal elements that represent masonry are modeled using the Corotational Truss element. The diagonal elements are modeled using the Corotational Truss2 element. The Truss element was used to model reinforcing steel present in masonry joints.

To obtain a better approximation of masonry response, non-linear models were calibrated with experimental data. Five masonry wall specimens tested in the laboratory were

considered: (1) M-0-E6 (Aguilar and Alcocer, 2001 [28]); (2) 421 (Treviño et al., 2004 [29]); (3) MB-0 (Cruz et al., 2015 [30]); (4) M-1/4-E6 (Aguilar and Alcocer, 2001 [28]); and (5) MB-3 (Cruz et al., 2015 [30]). Figure 6 illustrates specimen MB-3 (with horizontal reinforcement) and its corresponding beam-truss model.

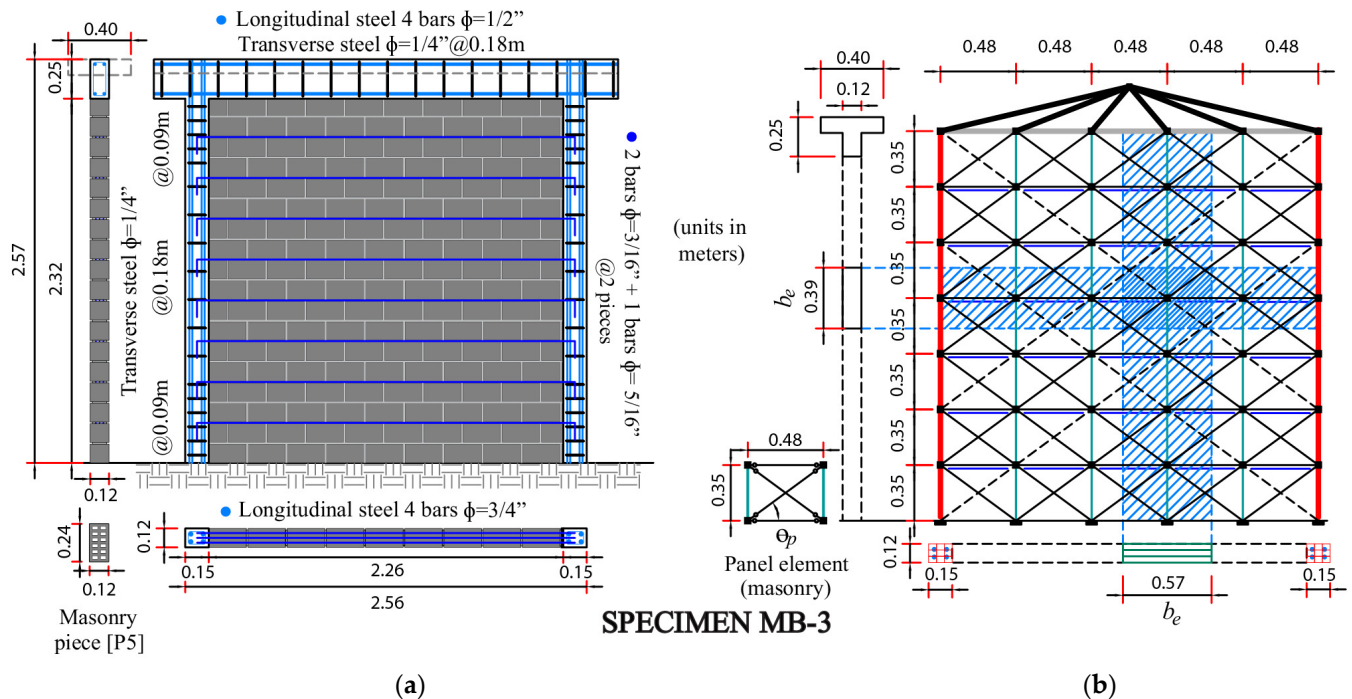


Figure 6. Modelling of confined masonry walls: (a) lab specimens; (b) beam-truss model.

A calibration process was empirically performed at the maximum resistance point of the stress–strain experimental curve. The stress–strain values corresponding to the post-maximum resistance states were validated considering three criteria: (a) no numerical instability in the beam-truss model due to the value of stress or strain; (b) the value of stress or strain that enables a reasonable approximation of experimental shear at the base of the wall; and (c) the value of stress or strain that permits the energy for each analytical cycle to coincide as much as possible with the energy in every experimental cycle. In the analytical models, the experimental values associated with the elastic and maximum strength states were maintained.

The research presented here establishes a level of refinement capable of analytically simulating the behavior of structural elements relevant to the lateral performance of the building. The results are presented in Figure 7, which shows a comparison between the analytical and experimental hysteretic curves, corresponding to the five specimens. It can be seen that the results of experimental hysteresis for masonry walls can be reasonably approximated using beam-truss modeling.

4.3. Seismic Motions

A total of 22 seismic motions recorded in Mexico City were selected to perform the Nonlinear Time History Analyses. Such records are historical, and most of them were registered during the 19 September 2017 earthquake (19S-2017), in the ground with a dominant period close to 1 s. Figure 8a shows the pseudo acceleration response spectra for a critical damping percentage of 5%. Such seismic motions were scaled according to the uniform hazard spectrum in an interval of interest as a function of the fundamental period of the building T_1 . The uniform hazard spectrum used in the present study has been developed by software associated with the Supplementary Technical Regulations for Mexican Seismic Design specifically for the construction site.

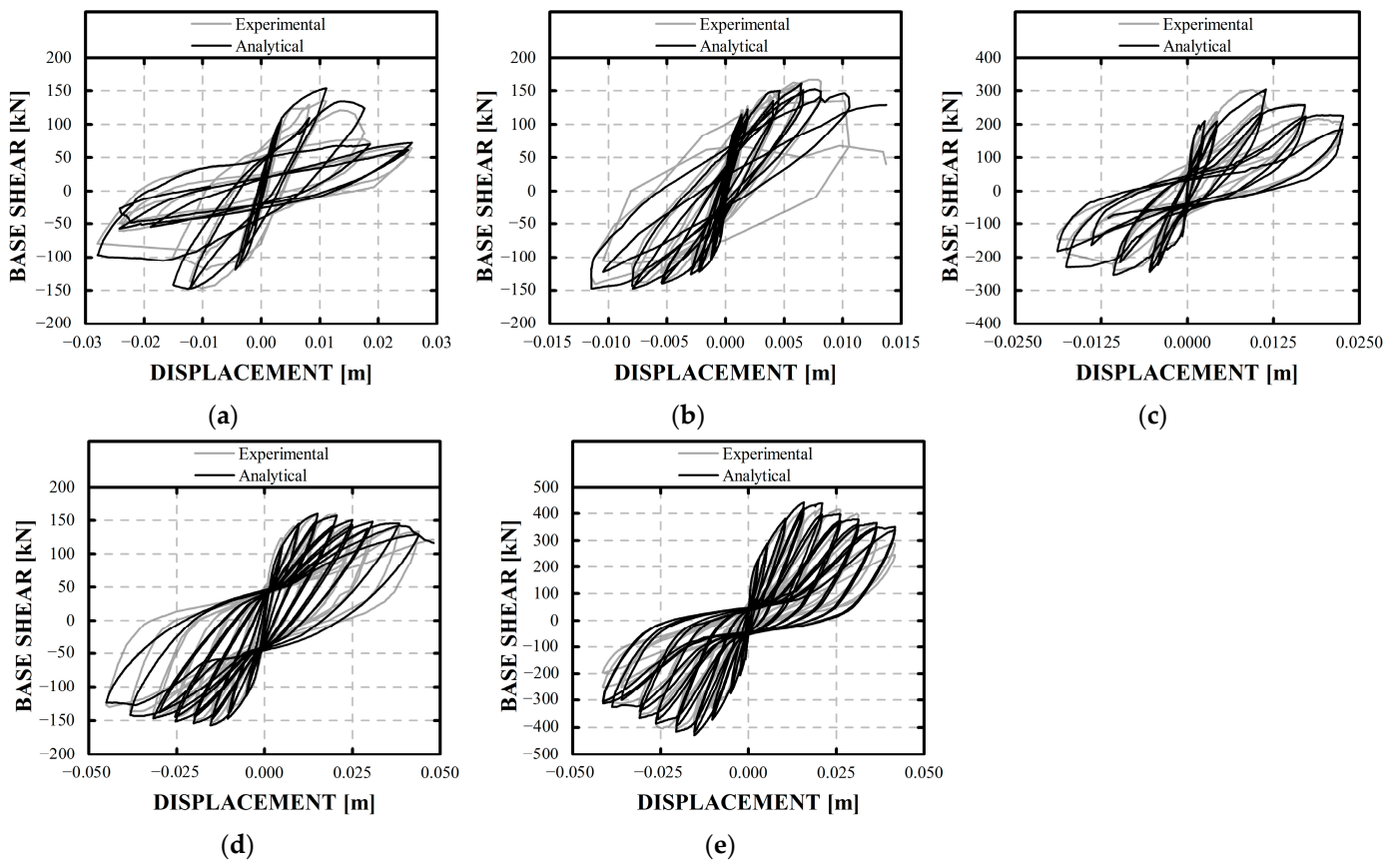


Figure 7. Analytical-experimental hysteretic curves: (a) M-0-E6; (b) 421; (c) MB-0; (d) M-1/4-E6; (e) MB-3.

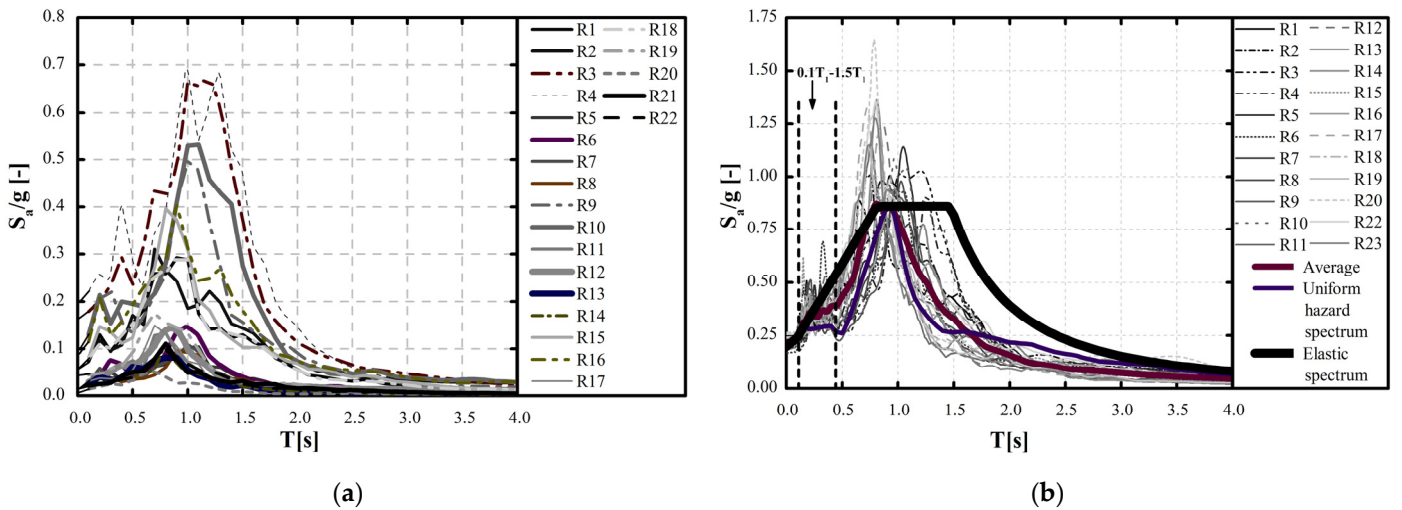


Figure 8. (a) Response spectra; (b) example of a scaled spectrum, $S_{avg}/g = 0.28$, associated with the three-story building.

There are several ways to scale the seismic ground motions [31–34]. Here, these were scaled in accordance with the Supplementary Technical Regulations for Mexican Seismic Design Guidelines, based on uniform hazard spectrum, with the average intensity measured S_{avg} [31] in an interval of interest between $0.1 T_1$ and $1.5 T_1$.

Figure 8b shows the response spectra of the 22 seismic motions scaled to a $S_{avg}/g = 0.28$ corresponding to $T_1 = 0.26$ s. Both the elastic design spectrum and the uniform hazard spectrum are also shown.

4.4. Condensation of MDOF Systems to Simplified 2EDOF Systems

In the second part of the methodology, the MDOF building is transformed into a two-dimensional global shear deformations-type structure, reducing the stiffness matrix to only consider a translational degree of freedom in the X direction (Figure 1e). To validate the bidimensional system, both the fundamental period of vibration T_n and mode shape profile $\{\varphi_n\}$ are compared with the corresponding values of the MDOF original system; these should be equal. Then, the matrices of mass $[M]$, stiffness $[K]$, and damping $[C]$ of the system are divided into two parts and substituted in Equations (9)–(11) to obtain the linear dynamic properties of the 2EDOF system, corresponding to the n -th vibration mode.

4.4.1. Linear Properties of the 2EDOF System

Matrices $\left[\tilde{M}\right]$ and $\left[\tilde{C}\right]$ are both obtained directly. However, the elastic stiffnesses k_{pn} and k_{bn} are obtained by equating matrix k (derived from a stiffness analysis with the 2EDOF system) to the elements of matrix $\left[\tilde{K}\right]$. Table 4 shows the most relevant linear properties of the simplified systems. The vibration periods, T , shown were calculated based on the expected concrete and masonry strengths; these values differ from those in Table 2, which correspond to nominal properties.

Table 4. Linear properties of the 2EDOF systems.

Case	Linear Properties	Three Story	Five Story	Seven Story
P1	$T(s)$	0.265	0.344	0.489
	l_{pn}, l_{bn}	1, -4.671	1, -1.801	1, -1.287
	k_{pn}, k_{bn}	26,451.58, 137,745.34	7248.92, 6247.10	2648.83, 766.60
	m_{pn}, m_{bn}	10.065, 3.310	11.967, 0.411	12.291, 0.068
	Hysteresis rule p_n	Hysteretic	Pinching4	Pinching4
	Hysteresis rule b_n	Pinching4	Hysteretic	Hysteretic
P2	$T(s)$	0.215	0.268	0.368
	l_{pn}, l_{bn}	1, -10.328	1, -3.674	1, -1.674
	k_{pn}, k_{bn}	108,084.70, 1,458,995.54	30,074.37, 88,224.35	7407.83, 5109.64
	m_{pn}, m_{bn}	12.118, 4.893	14.634, 1.032	15.250, 0.139
	Hysteresis rule p_n	Hysteretic	Pinching4	Pinching4
	Hysteresis rule b_n	Pinching4	Hysteretic	Hysteretic
P3	$T(s)$	0.194	0.230	0.293
	l_{pn}, l_{bn}	1, -12.610	1, -5.109	1, -2.204
	k_{pn}, k_{bn}	135,028.39, 2,323,906.77	46,726.45, 218,211.46	13,615.12, 17,045.47
	m_{pn}, m_{bn}	10.018, 4.449	12.280, 1.346	13.359, 0.285
	Hysteresis rule p_n	Hysteretic	Hysteretic	Pinching4
	Hysteresis rule b_n	Pinching4	Pinching4	Hysteretic
P4	$T(s)$	0.264	0.355	0.504
	l_{pn}, l_{bn}	1, -3.731	1, -1.690	1, -1.221
	k_{pn}, k_{bn}	21,765.02, 82,860.15	6404.66, 4770.45	2331.13, 528.17
	m_{pn}, m_{bn}	10.273, 2.962	11.992, 0.382	12.297, 0.055
	Hysteresis rule p_n	Hysteretic	Pinching4	Pinching4
	Hysteresis rule b_n	Pinching4	Hysteretic	Hysteretic
P5	$T(s)$	0.257	0.266	0.314
	l_{pn}, l_{bn}	1, -23.569	1, -10.201	1, -3.878
	k_{pn}, k_{bn}	154,026.61, 5,095,370.09	67,493.73, 736,079.20	20,516.173, 62,158.648
	m_{pn}, m_{bn}	10.920, 4.870	11.892, 1.989	13.053, 0.509
	Hysteresis rule p_n	Hysteretic	Hysteretic	Pinching4
	Hysteresis rule b_n	Pinching4	Pinching4	Hysteretic

It is considered that the two first vibration modes in the direction of the analysis are sufficient to approximate the response of the MDOF systems studied herein.

4.4.2. Behavior of the 2EDOF Simplified System

The selection of Case I or II depends on the subsystem that presents the Maximum Interstory Drift Index (MIDI). As a result of Modal Nonlinear Pushover Analyses performed on the MDOF systems, Figures 9–11 illustrates the MIDI profiles associated with the Collapse Prevention Limit State. This a performance level proposed by the Supplementary Technical Regulations for Mexican Seismic Design related to building collapse. Its definition corresponds to the drift that exceeds the Maximum Permissible Interstory Drift Index. Therefore, MIDI (Table 2) is considered to be the acceptance criteria for the global building response for this limit state.

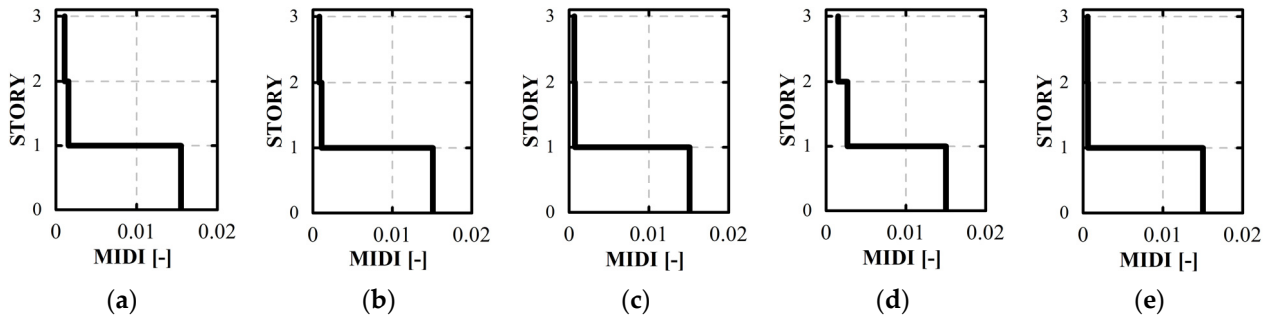


Figure 9. MIDI profiles of three-story buildings for the following cases: (a) P1; (b) P2; (c) P3; (d) P4; (e) P5.

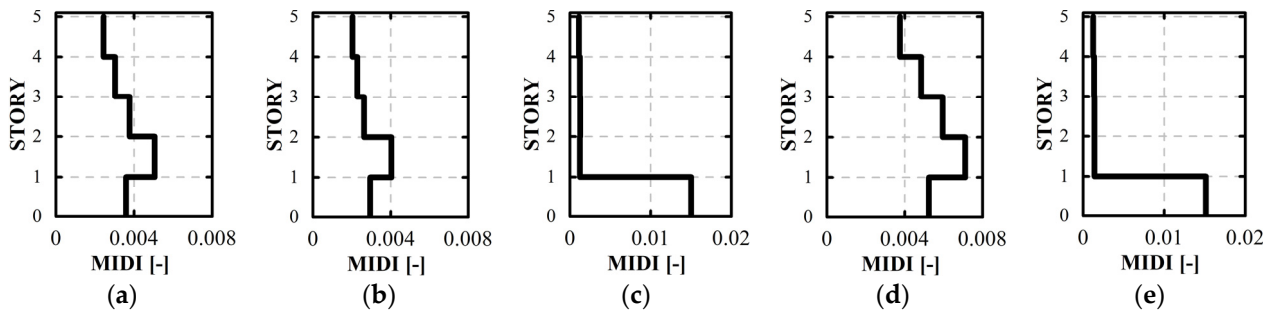


Figure 10. MIDI profiles of five-story buildings for the following cases: (a) P1; (b) P2; (c) P3; (d) P4; (e) P5.

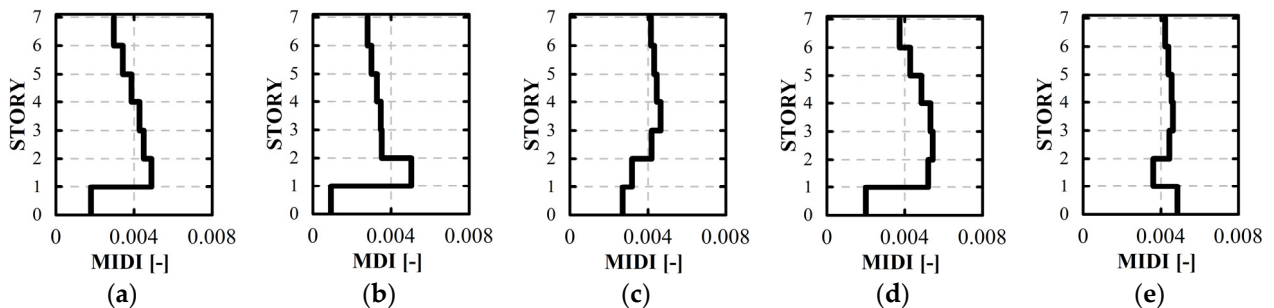


Figure 11. MIDI profiles of seven-story buildings for the following cases: (a) P1; (b) P2; (c) P3; (d) P4; (e) P5.

The pattern of lateral load corresponds to the first mode shape in the X direction. The results for the cases studied are summarized in Table 5.

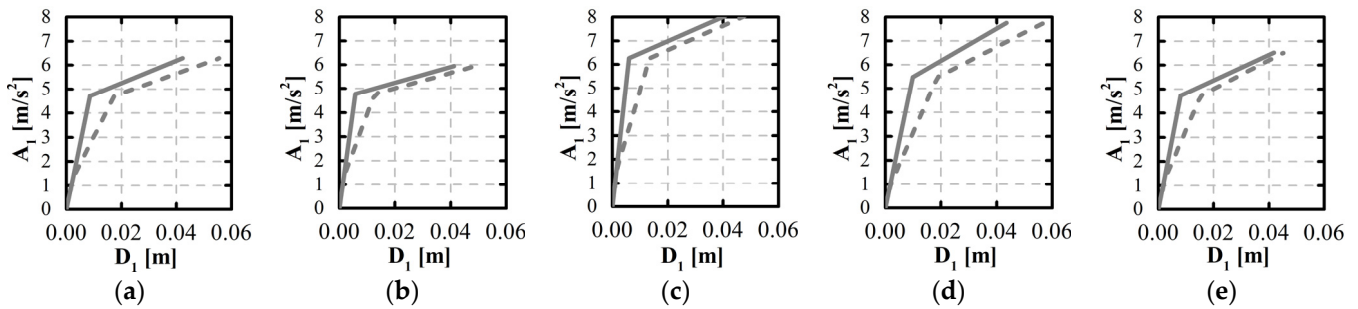
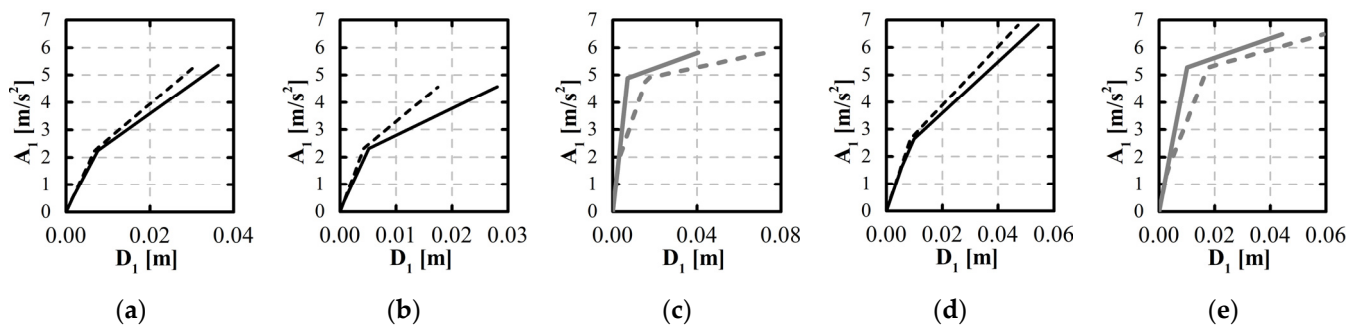
Table 5. Cases corresponding to the non-linear behavior of the 2EDOF system.

Stories	P1	P2	P3	P4	P5
3	II	II	II	II	II
5	I	I	II	I	II
7	I	I	I	I	I

In most MIDI profiles, a specific case is clearly illustrated. For example, in the selection of behavior P3 (Figure 11c) for the seven-story building, the masonry wall fails before the reinforced concrete frames, corresponding to Case I.

4.4.3. Non-Linear Properties of the 2EDOF System

The non-linear properties of the simplified 2EDOF system, which are calculated with the idealized capacity curves, are different depending on the Case (I or II). According to Figure 1(k), the idealized curves are built as a function of the capacity curves $A_n - D_n$ in spectral format (Equation (12)), which are derived from the $V_B - d_n$ capacity curves, obtained from the Modal Nonlinear Pushover Analyses performed on the MDOF systems. Figures 12–14 show the cases of $A_n - D_n$ idealized curves in both bilinear and trilinear formats for the first vibration mode considered. $A_n - D_n$ curves that represent the US are shown with a continuous line, whereas the dotted line represents the BS curves. To distinguish behavior cases (Table 5), a black curve represents Case I, and in grey is the curve representing Case II.

**Figure 12.** Idealized capacity curves for a three-story MDOF system for the following cases: (a) P1; (b) P2; (c) P3; (d) P4; (e) P5.**Figure 13.** Idealized capacity curves for a five-story MDOF system for the following cases: (a) P1; (b) P2; (c) P3; (d) P4; (e) P5.

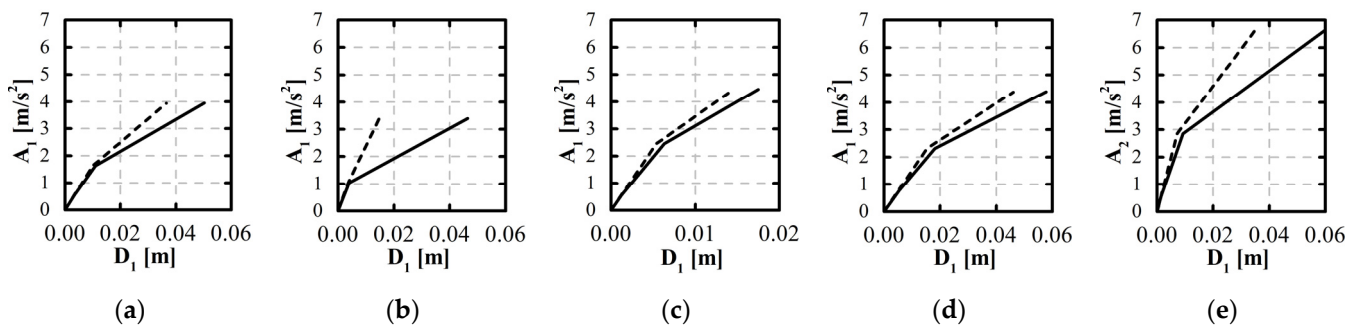


Figure 14. Idealized capacity curves for a seven-story MDOF system for the following cases: (a) P1; (b) P2; (c) P3; (d) P4; (e) P5.

Figures 12–14 show that relations $A_n - D_{pn}$ and $A_n - D_{bn}$ superpose at the beginning, which indicates that both the reinforced concrete frames and the masonry walls remain elastic. Thus, up to this point, it is possible to calculate the response by means of a 1EDOF system. Then, the curves are divided, showing that displacements D_{pn} and D_{bn} are no longer the same, meaning that one of the two subsystems presents nonlinearity, so the 1EDOF system is no longer adequate to calculate the response at this stage.

The methodology employed in the present study considers that in buildings like those studied here, an OGS-WFS or an OGS-WSS mechanism occurs depending on the lateral shear resistance value and the deformation capacity of masonry compared to that of concrete frames when the number of levels exceeds three. The prediction of these mechanisms can be readily determined by means of capacity curves such as those shown in Figures 12–14, regardless of the building's complexity. Notice that when the BS (dotted line) yields first, the mechanism corresponds to a WFS; on the other hand, if the US (continuous line) yields first or nearly simultaneously with the BS, the mechanism corresponds to a WSS. For buildings with other materials, more complex structural distributions and/or more levels, the choice of the mechanisms must be made based on Modal Nonlinear Pushover Analysis, considering all elements that can significantly contribute to lateral resistance.

4.4.4. Analysis of the Hysteretic Behavior of the Simplified 2EDOF System

Figure 15 shows the moment–rotation $M - \theta$ hysteresis cycles of both rotational springs of the 2EDOF system. The hysteresis curves correspond to the most representative responses shown in Figures 16–18. For each case (masonry type), the figure shows, from left to right, the curves associated with the first and second vibration modes. The hysteresis curve for the upper spring pn is shown in grey, and the curve for the lower spring bn is shown in black.

In Figure 15a,b, the lower spring bn (BS) reaches the non-linear interval in the first mode, whereas the upper spring pn (US) remains linear. As will be seen below, Figures 19 and 20 indicate that the MIDI in MDOF systems is present in the OGS. That is, the maximum seismic lateral deformation is concentrated in the OGS. Therefore, the behavior of the spring bn (BS) that represents the OGS in the hysteresis curves is reasonable.

Figure 15c displays the hysteresis cycles of the seven-story 2EDOF system. It is observed that, in the first mode, the hysteresis rule used in the upper spring pn of case P1 shows the drop in strength through a negative slope (which denote the hysteretic rule with strength degradation). This is because such rule establishes a point at which the spring no longer increases its strength, unlike the bilinear rules. The use of a bilinear rule implies that strength may become infinite at very high rotation values; however, such behavior is not considered by the MDOF systems studied herein.

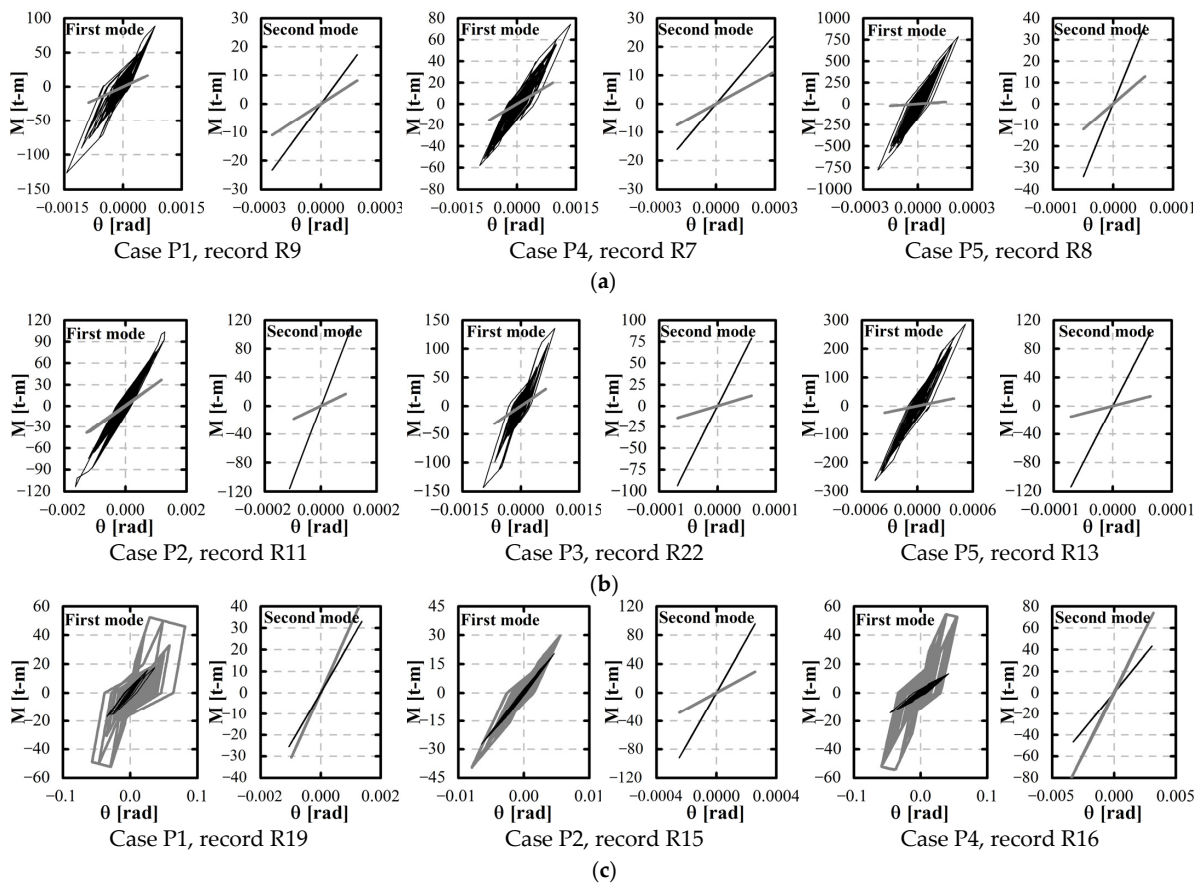


Figure 15. Hysteresis curves of the rotational springs in the 2EDOF system: (a) three-story, (b) five-story; (c) seven-story building.

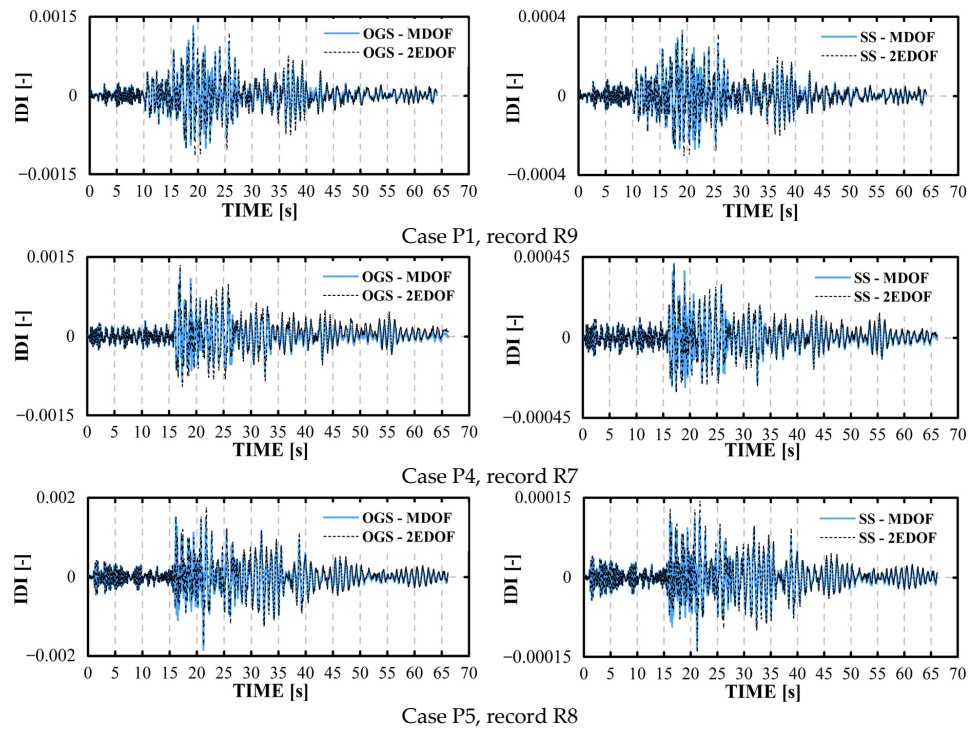


Figure 16. IDI histories for three-story systems.

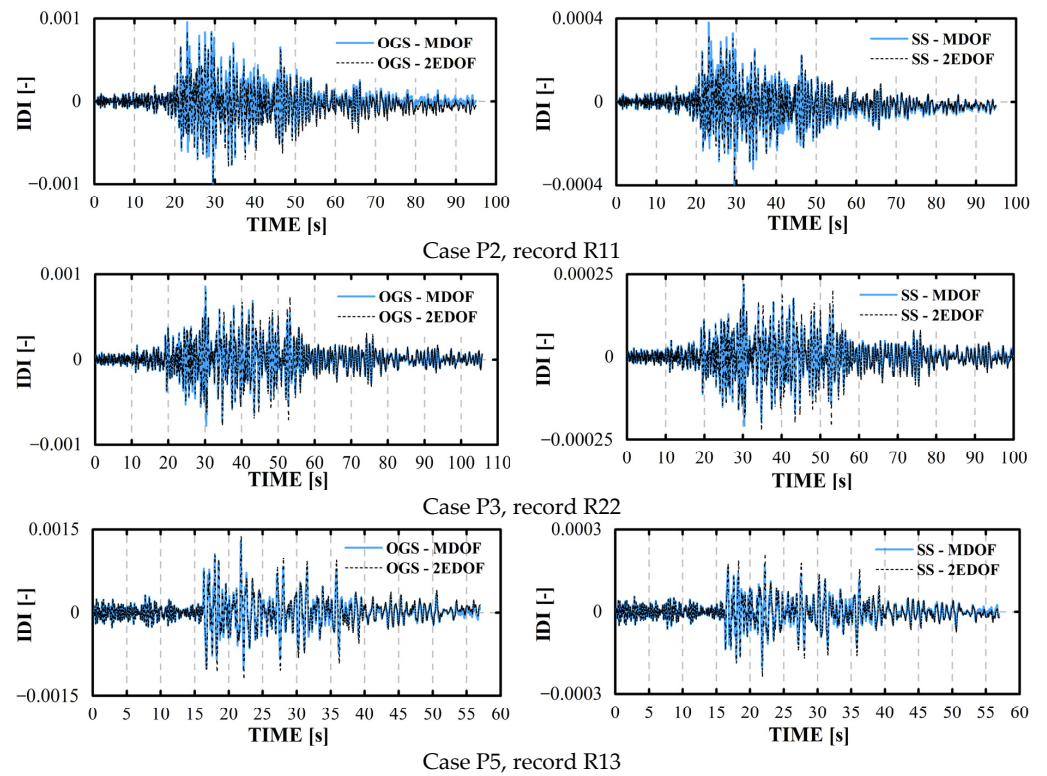


Figure 17. IDI histories for five-story systems.

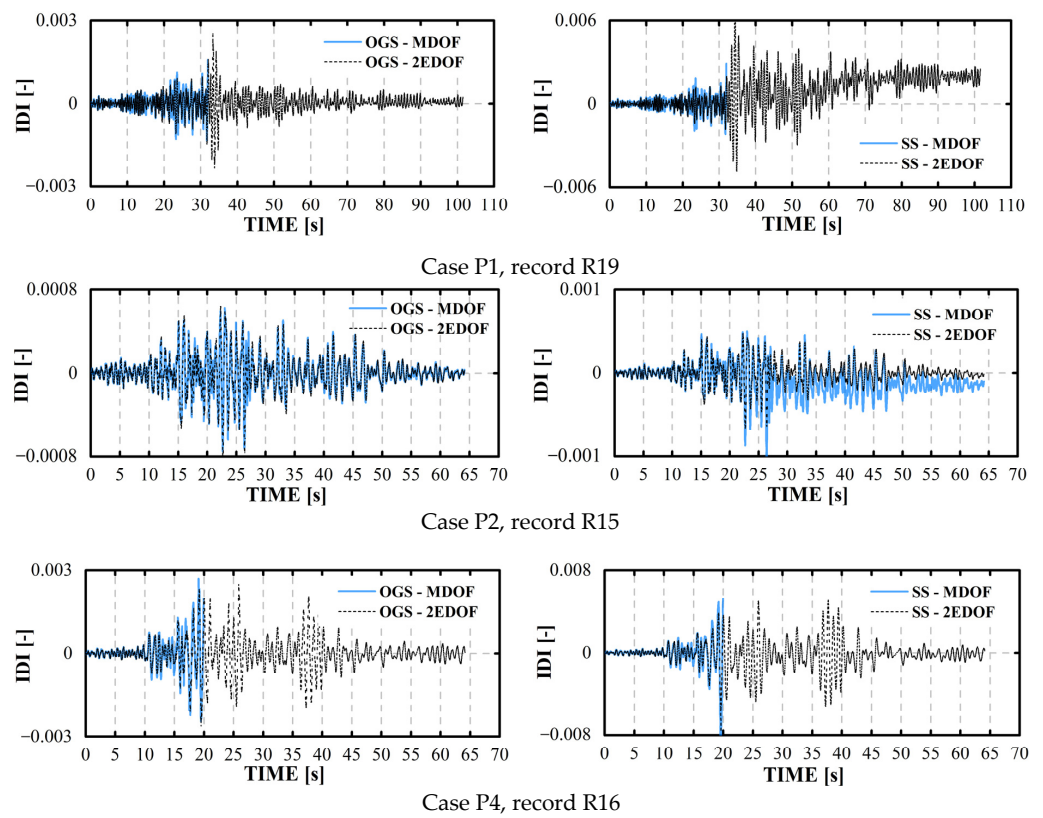


Figure 18. IDI histories for seven-story systems.

It is highlighted that in all cases, the response is dominated by the 2EDOF system associated with the first mode. Therefore, the 2EDOF system behavior for the second mode is elastic. This is due to two aspects: (a) T_1 has a higher spectral ordinate than T_2 (see

Figure 6b); and (b) T_1 moves more seismic mass than T_2 , as indicated by its participation Mass Ratios shown in Table 2.

4.5. Comparison between the Responses of the MDOF Systems and the 2EDOF Systems

This section deals with the third part of the methodology shown in Figure 1. A series of Nonlinear Time History Analyses is done using the 2EDOF systems, and the seismic motions previously mentioned. The response in terms of story Interstory Drift Index history is examined first, as shown in Figures 16–18, which display both the MDOF system and the 2EDOF system responses. The history on the left corresponds to the open ground story, and the history on the right is for the second story (SS). The histories shown are the most representative in each case.

Figures 16–18 indicate that, in most cases, the 2EDOF system reasonably approximates maximum IDI values. The MDOF system histories shown in Figure 18 the cases P1 and P4 show an abrupt ending in the IDI history. As a result of the seismic demand exceeding the capacity of the beam-truss elements, some panel elements were disconnected from the main structure on the second story; this resulted in the OpenSees software failing to converge and terminating the analysis. Hence, it is concluded that the simplified 2DOF system has the limitation of not approximating the response of MDOF systems when they present a local failure in the story, showing IDI values for instants of time greater than the instant of time associated with the local failure of the MDOF system, as displayed in Figure 17.

Figures 19–21 show the validation of the 2EDOF systems. These are categorized according to the type of masonry used and to the number of building levels. In each case, the figure on the left corresponds to the Maximum Interstory Drift Index (MIDI) profile, and the figure on the right corresponds to the error margin obtained in model validation. These profiles are called $MIDI_N$ profiles.

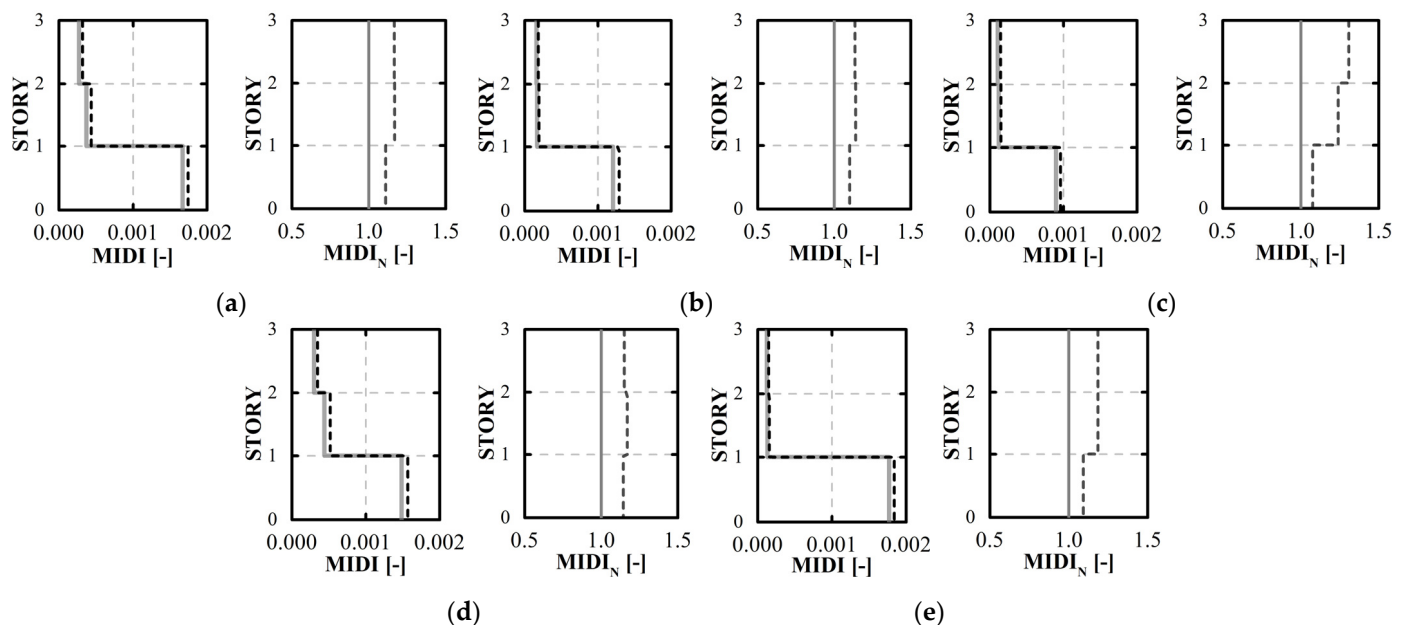


Figure 19. Comparison of MIDI profiles of MDOF and 2EDOF systems. Left: average MIDI profile. Right: normalized average MIDI profile. Number of stories: three stories. Cases: (a) P1; (b) P2; (c) P3; (d) P4; (e) P5.

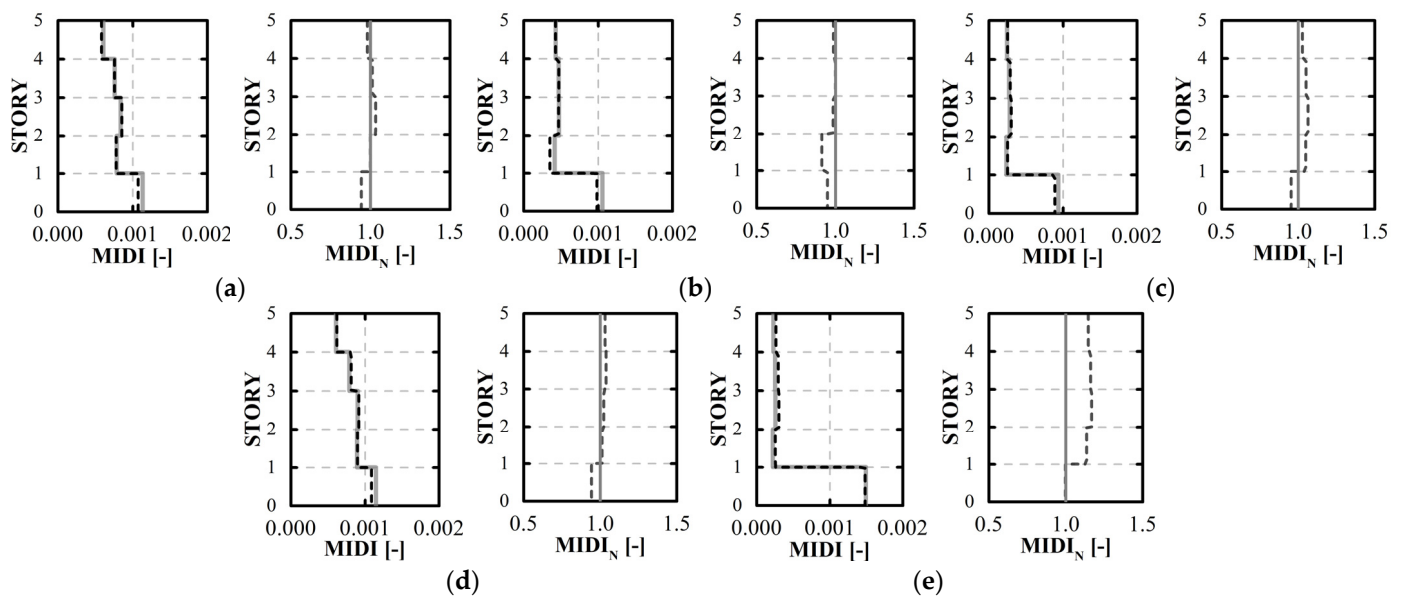


Figure 20. Comparison of MIDI profiles of MDOF and 2EDOF systems. Left: average MIDI profile. Right: normalized average MIDI profile. Number of stories: five stories. Cases: (a) P1; (b) P2; (c) P3; (d) P4; (e) P5.

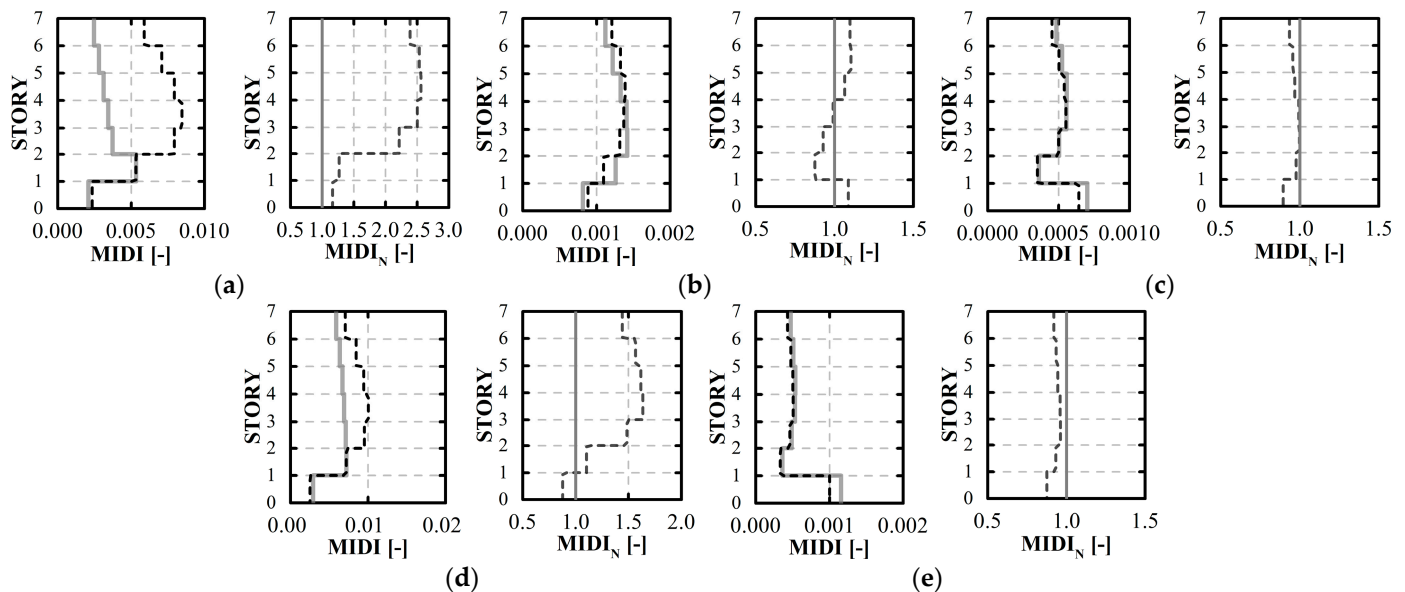


Figure 21. Comparison of MIDI profiles of MDOF and 2EDOF systems. Left: average MIDI profile. Right: normalized average MIDI profile. Number of stories: seven stories. Cases: (a) P1; (b) P2; (c) P3; (d) P4; (e) P5.

MIDI profiles are constructed using the response obtained from the Nonlinear Time History Analyses performed using the 22 seismic records scaled with respect to their design intensity. The Maximum Interstory Drift Index is used as a global response indicator, calculated as the average of the individual responses from seismic records. In the MIDI profiles, the 2EDOF system's response is represented by a continuous gray line, and the MDOF system's response by a dotted black line.

MIDI_N profile is constructed by normalizing the 2EDOF system's response with respect to that of MDOF and corresponds to the average of the normalized ratios of each seismic record. In each figure, the black dashed line represents the MIDI_N average profiles, and in each case, the continuous gray line provides a unitary benchmark to gauge the error extent

in the simplified response. When the average values are close to the benchmark, the 2EDOF system's response is the same as that of the MDOF system. On the other hand, an average value far from 1 represents a large difference in the individual response per seismic record.

The MIDI profiles show that the scenarios corresponding to cases WFS and OGF-WSS are successfully reproduced by the simplified 2EDOF system. The simplified system studied adequately reproduces the drastic Interstory Drift Index change between the ground story and the second story. However, for cases P1 and P4, with seven stories, and case I, the simplified system can only approximate the IDI of both the ground story and the second story, as seen in Figure 21a,d. Such figures also show that, in their corresponding IDI profiles, the degree of freedom assigned to the US does not consider the scenario in which a story presents an IDI demand considerably greater than the rest of the stories do; that is, the modal superposition approach of the simplified system does not reproduce the changes in the lateral strength of its stories because the US response is obtained as the product of displacement D_{pn} calculated through an elastic modal form, similarly to that in a 1EDOF system.

Generally, the shape of the lateral deflection observed by the 2EDOF system is consistent with the requirements established by the MDOF system. Although there is a certain variation in an individual record's response at the upper stories, the MIDI and MIDI_N profiles clearly demonstrate a high level of precision at the first and second stories.

5. Future Studies Applying the Proposed Methodology

A parametric analysis is currently being conducted at the National Autonomous University of Mexico using 2EDOF systems which represent the lateral behavior of mid-rise buildings with OGS that could fail due to OGS-WFS or OGS-WSS. In the future, it is planned to propose guidelines for the design of these type of buildings. The studies are oriented to the following:

- Improve the knowledge about the influence of stiffness and lateral strength ratios, considering an extended classification range.
- Establish lateral deformation limits considering stiffness and strength ratios supported by predictive seismic demand analysis, using 2EDOF simplified systems.
- Include axial load level control at the first story to avoid premature instability of the OGS-WFS systems.
- Limit the maximum ductility capacity of the OGS building in response to a specified seismic intensity.

In summary, the guidelines would increment the constraints in the practical design of mid-rise buildings with OGS constituted by masonry walls and concrete frames, in order to enhance their seismic performance.

6. Conclusions

An improved methodology for condensing Multi-Degree-Of-Freedom buildings with Open Ground Story has been proposed and successfully applied to obtain simplified Two-Equivalent-Degree-Of-Freedom systems. The systems studied herein approximate, under certain restrictions, the behavior of buildings with vertical irregularities. These buildings are susceptible to developing either an OGS-WFS or an OGS-WSS. It is noticed that the non-linear analysis of such buildings structured with different masonry types and different number of stories, located in Mexico City, had not been studied in detail before.

The main contributions of this study are the following:

1. The demand for non-linear behavior in buildings with OGS does not always occur on the ground story. The Nonlinear Time History Analyses showed that both the linear and non-linear structural properties used in the upper stories influence the lateral behavior of the ground story. It also shows the impact that the properties of the masonry used in the upper stories may have on the seismic response of OGS buildings. This makes evident the fact that the failure mode may be different from a WFS building, depending on the linear and/or non-linear structural properties and on the number of stories in the building. In most of the buildings analyzed, the MIDI is

- not exceeded; however, the results obtained for a seven-story building structured with low-strength masonry clearly indicate that when the design focuses on OGS behavior, it can underestimate the seismic demand in the upper stories. So, it is recommended to perform Nonlinear Time History Analyses in tall buildings with vertical irregularities.
2. The use of hysteresis rules with degradation of both stiffness and strength in the rotational springs of the 2EDOF system allows it to adequately approximate the behavior of OGS-WSS and OGS-WFS cases corresponding to MDOF systems. The application of a descending branch in the hysteretic rule to define the ultimate state in the spring that displays the greatest Interstory Drift Index contributes considerably to approximate the seismic response of masonry walls or reinforced concrete structures under high seismic intensities.
 3. The responses of the 2EDOF systems obtained from Nonlinear Time History Analyses satisfactorily reproduce the drastic change in Interstory Drift Index between the ground story and the second story. Likewise, such responses reasonably capture the migration of the Interstory Drift Index from the ground story to the second story as seismic intensity increases; however, the 2EDOF simplified model has the following limitations: (a) the maximum nonlinearity is located in the first or in the second degree of freedom, not in both; (b) it is incapable of reproducing the local failure of MDOF system elements; (c) the simplified US system is unable to reproduce the evolution of the damage on the different stories; (d) because the response of the simplified systems is governed by the non-linear behavior of the interstory, they cannot approximate the response to excessive in-plane torsion; and (e) a failure mechanism in the OGS does not damage the stories above it.
 4. The local failure observed in the Interstory Drift Index profiles of seven-story buildings P1 and P4 represents a mechanism that impacts the limits of application of the improved methodology. The response in these buildings cannot be adequately approximated by the 1EDOF nor the 2EDOF systems. Therefore, the results derived from the application of this methodology in real buildings whose behavior is governed by this type of failure must be approached with caution.
 5. The simplified 2DOF model is permitted to be applied only in cases where no significant local interstory failure has occurred due to a certain level of seismic demand. It is noticed that the 2DOF simplified model demonstrates reasonable accuracy in predicting two mechanisms: (a) OGS-WFS, and (b) OGS-WSS, and that the model is inadequate when the Maximum Interstory Drift Index is concentrated above the second story.

Author Contributions: Conceptualization, J.L.C. and S.E.R.; methodology, J.L.C., S.E.R. and A.T.-G.; software, J.L.C. and A.T.-G.; validation, S.E.R. and A.T.-G.; formal analysis, J.L.C.; investigation, J.L.C. and S.E.R.; resources, S.E.R.; data curation, J.L.C.; writing—original draft preparation, S.E.R.; writing—review and editing, J.L.C., S.E.R. and A.T.-G.; visualization, S.E.R. and A.T.-G.; supervision, S.E.R. and A.T.-G.; project administration, S.E.R.; funding acquisition, J.L.C. and S.E.R. All authors have read and agreed to the published version of the manuscript.

Funding: The authors thank the support received from the DGAPA-UNAM within the project PAPIIT-IN100423. This research work was developed with the economic support provided by the National Council of Humanities, Science and Technology (CONAHCYT) to the first author, during his graduate studies.

Data Availability Statement: The data used to support the findings of this study are available from the corresponding author upon request.

Acknowledgments: The authors thank S. M. Alcocer, J. J. Pérez Gavilán and A. I. Cruz Olayo, for providing the experimental data of the confined masonry specimens; and the Center for Seismic Recording and Instrumentation (CIRES, for its acronym in Spanish), for providing the seismic records used in the study. The first author thanks the National Council of Humanities, Science and Technology (CONAHCYT, acronym in Spanish), for the support provided during his graduate studies.

Conflicts of Interest: The authors declare no conflicts of interest.

References

1. Chintanapakdee, C.; Chopra, A.K. Seismic Response of Vertically Irregular Frames: Response History and Modal Pushover Analyses. *J. Struct. Eng.* **2004**, *130*, 1177–1185. [[CrossRef](#)]
2. Al-Ali, A.A.K. *Effects of Vertical Irregularities on Seismic Behavior of Building Structures*; Stanford University: Stanford, CA, USA, 1998.
3. Michalis, F.; Dimitrios, V.; Manolis, P. Evaluation of the influence of vertical irregularities on the seismic performance of a nine-storey steel frame. *Earthq. Eng. Struct. Dyn.* **2006**, *35*, 1489–1509. [[CrossRef](#)]
4. Valmundsson, E.V.; Nau, J.M. Seismic response of building frames with vertical structural irregularities. *J. Struct. Eng.* **1997**, *123*, 30–41. [[CrossRef](#)]
5. Ruiz, S.E.; Diederich, R. The Mexico Earthquake of September 19, 1985—The Seismic Performance of Buildings with Weak First Storey. *Earthq. Spectra* **1989**, *5*, 89–102. [[CrossRef](#)]
6. Esteva, L. Nonlinear seismic response of soft-first-story buildings subjected to narrow-band accelerograms. *Earthq. Spectra* **1992**, *8*, 373–389. [[CrossRef](#)]
7. Fajfar, P.; Gašperšič, P. The N2 method for the seismic damage analysis of RC buildings. *Earthq. Eng. Struct. Dyn.* **1996**, *25*, 31–46. [[CrossRef](#)]
8. Dolšek, M.; Fajfar, P. Simplified probabilistic seismic performance assessment of plan-asymmetric buildings. *Earthq. Eng. Struct. Dyn.* **2007**, *36*, 2021–2041. [[CrossRef](#)]
9. Ruggieri, S.; Chatzidakis, A.; Vamvatsikos, D.; Uva, G. Reduced-order models for the seismic assessment of plan-irregular low-rise frame buildings. *Earthq. Eng. Struct. Dyn.* **2022**, *51*, 3327–3346. [[CrossRef](#)]
10. Lin, J.L.; Tsai, K.C. Simplified seismic analysis of asymmetric building systems. *Earthq. Eng. Struct. Dyn.* **2007**, *36*, 459–479. [[CrossRef](#)]
11. Bakalis, K.; Fragiadakis, M.; Vamvatsikos, D. Surrogate modelling of liquid storage tanks for seismic performance design and assessment. In Proceedings of the 5th ECCOMAS Thematic Conference on Computational Methods in Structural Dynamics and Earthquake Engineering, Crete Island, Greece, 25–27 May 2015. [[CrossRef](#)]
12. Kuramoto, H.; Teshigawara, M.; Lkuzono, T.; Koshika, N.; Takayama, M.; Hori, T. Predicting the earthquake response of buildings using equivalent single degree of freedom system. In Proceedings of the 12th World Conference on Earthquake Engineering, Auckland, New Zealand, 30 January–4 February 2000. Paper No. 1039.
13. Xu, L.; Yuan, X.L. A simplified seismic design approach for mid-rise buildings with vertical combination of framing systems. *Eng. Struct.* **2015**, *99*, 568–581. [[CrossRef](#)]
14. Tena-Colunga, A.; Hernández-García, D.A. Peak seismic demands on soft and weak stories models designed for required code nominal strength. *Soil Dyn. Earthq.* **2020**, *129*, 105698. [[CrossRef](#)]
15. Lin, J.L.; Tsaur, C.C.; Tsai, K.C. Two-degree-of-freedom modal response history analysis of buildings with specific vertical irregularities. *Eng. Struct.* **2019**, *184*, 505–523. [[CrossRef](#)]
16. Mazzoni, S.; McKenna, F.; Scott, M.H.; Fenves, G.L. *OpenSees Command Language Manual*; Pacific Earthquake Engineering Research (PEER) Center: Berkeley, CA, USA, 2006; Volume 264, pp. 137–158.
17. MCBC. *Mexico City Building Code*; Government of Mexico City: Mexico City, Mexico, 2017.
18. Mexico City Government. *Normas Técnicas Complementarias para Diseño por Sismo*; Gaceta Oficial de la Ciudad de México: Mexico City, Mexico, 2020. (In Spanish)
19. Zúñiga Cuevas, O.; Terán Gilmore, A. Evaluación basada en desplazamientos de edificaciones de mampostería confinada. *Rev. Ing. Sísmica* **2008**, *79*, 25–48. [[CrossRef](#)]
20. Ezequiel, A. Predicción de Las Capacidades de Resistencia a Flexocompresión Y de Desplazamiento Lateral de Columnas de Concreto Presforzado en Zona Sísmicas. Master's Thesis, Universidad Autónoma Nacional de México, Mexico City, Mexico, 2015.
21. Mander, J.B.; Priestley, M.J.N.; Park, R. Theoretical stress-strain model for confined concrete. *J. Struct. Eng.* **1988**, *114*, 1804–1826. [[CrossRef](#)]
22. Rodríguez, M.; Botero, C. *Aspectos Del Comportamiento Sísmico de Estructuras de Concreto Reforzado Considerando Las Propiedades Mecánicas de Aceros de Refuerzo Producidos En México*; II-UNAM: Mexico City, Mexico, 1996; Volume 1.
23. Lu, Y.; Panagiotou, M. Three-dimensional cyclic beam-truss model for nonplanar reinforced concrete walls. *J. Struct. Eng.* **2014**, *140*, 04013071. [[CrossRef](#)]
24. Lu, Y.; Panagiotou, M.; Koutromanos, I. *Three-Dimensional Beam-Truss Model for Reinforced-Concrete Walls and Slabs Subjected to Cyclic Static or Dynamic Loading*; Report No. PEER 2014/18; Pacific Earthquake Engineering Research Center: Berkeley, CA, USA, 2014.
25. Williams, S.A. Numerical Analysis of Reinforced Masonry Shear Walls Using the Nonlinear Truss Approach. Ph.D. Thesis, Virginia Tech, Blacksburg, VA, USA, 2014.
26. Ayala, M.C. Comportamiento Cíclico de Albañilería Armada de Bloques de Hormigón Parcialmente Relleno: Análisis Experimental Y Numérico. Master's Thesis, Pontificia Universidad Católica de Chile, Santiago de Chile, Chile, 2016.
27. Moharrami, M.; Koutromanos, I.; Panagiotou, M. Nonlinear truss modeling method for the analysis of shear failures in reinforced concrete and masonry structures. In *Improving the Seismic Performance of Existing Buildings and Other Structures 2015*; American Society of Civil Engineers: Reston, VA, USA, 2015; pp. 74–85. [[CrossRef](#)]
28. Aguilar, G.; Alcocer, S.M. *Efecto del Refuerzo Horizontal en el Comportamiento de Muros de Mampostería Confinada ante Cargas Laterales*; Universidad Nacional Autónoma de México: Mexico City, Mexico, 2001. (In Spanish)

29. Treviño, E.; Alcocer, S.M.; Flores, L.E.; Larrúa, R.; Zárate, J.M.; Gallegos, L. Investigación Experimental del Comportamiento de Muros de Mampostería Confinada de Bloques de Concreto Sometidos a Cargas Laterales Cíclicas Reversibles Reforzados con Acero Grados 60 y 42. In Proceedings of the Memorias XIV Congreso Nacional de Ingeniería Estructural, Acapulco, Mexico, 29 October–1 November 2004. (In Spanish)
30. Cruz, O.A.I.; Perez Gavilan, J.J.; Flores, C.L. Experimental study of in-plane shear strength of confined concrete masonry walls with joint reinforcement. *Eng. Struct.* **2019**, *182*, 213–226. [[CrossRef](#)]
31. Baker, J.; Cornell, C. Spectral shape, epsilon and record selection. *Earthq. Eng. Struct. Dyn.* **2006**, *35*, 1077–1095. [[CrossRef](#)]
32. Bojórquez, E.; Iervolino, I.; Reyes-Salazar, A.; Ruiz, S.E. Comparing vector-valued intensity measures for fragility analysis of steel frames in the case of narrow-band ground motions. *Eng. Struct.* **2012**, *45*, 472–480. [[CrossRef](#)]
33. Shome, N. Probabilistic Seismic Demand Analysis of Nonlinear Structures. Ph.D. Thesis, Department of Civil Engineering, Stanford University, Stanford, CA, USA, 1999.
34. Cordova, P.P.; Deierlein, G.G.; Mehanny, S.S.; Cornell, C.A. Development of a two-parameter seismic intensity measure and probabilistic assessment procedure. In Proceedings of the Second US–Japan Workshop on Performance-Based Earthquake Engineering Methodology for Reinforced Concrete Building Structures, Sapporo, Hokkaido, 11–13 September 2001; pp. 187–206.

Disclaimer/Publisher’s Note: The statements, opinions and data contained in all publications are solely those of the individual author(s) and contributor(s) and not of MDPI and/or the editor(s). MDPI and/or the editor(s) disclaim responsibility for any injury to people or property resulting from any ideas, methods, instructions or products referred to in the content.